CHARACTERIZING THE INTRACELLULAR STRATEGY OF *CRYPTOCOCCUS GATTII* WITHIN MACROPHAGES

by
Joudeh Bishara Freij

A thesis submitted to Johns Hopkins University with the requirements for the degree of Master of Science

Baltimore, Maryland
April 2017

Abstract

Cryptococcus gattii (Cg) can cause life-threatening disease in immunocompetent patients. *C. gattii*, unlike the sister species, *C. neoformans* (Cn), induces a less protective immune response in the host. We were interested in further examining the capsule of *C. gattii* and understanding its intracellular pathogenic strategy within macrophages.

To examine the capsule, capsular and exopolysaccharide were collected from one strain of *C. neoformans* (H99) and one strain of *C. gattii* (R265). Differences in binding of monoclonal antibodies to glucuronoxylomannan (GXM) of the polysaccharide was determined using ELISA. To understand and further characterize the intracellular strategy, the interaction between macrophages and three *C. gattii* strains (R265, WM179, and WM161) and one *C. neoformans* strain (H99) was analyzed by measuring phagocytosis frequency using light microscopy, non-lytic exocytosis using time-lapse microscopy, phagolysosomal pH by dual-excitation ratio fluorescent microscopy, and phagolysosomal membrane permeabilization by flow cytometry. Nitric oxide production was determined using the Griess reaction and a microplate assay.

For all the anti-GXM monoclonal antibodies tested, binding was less in the *C. gattii* GXM fractions as compared to *C. neoformans.* Capsule size in *C. gattii* strain WM179 was the largest in both Sabouraud Dextrose Broth and Minimal Media. Phagocytosis frequency was similar among all strains. Phagolysosomal pH over 24 hours was greatest in *C. neoformans* H99 infected BMDM, though from 0 to 4 hours, the pH was relatively similar between all strains. In infected J774 cells, apoptosis was greater in *C. gattii* R265 and *C. gattii* WM179 infections. Phagolysosomal membrane permeabilization also occurred in more cells infected with *C. gattii* R265 and *C. gattii* WM179 than with *C. neoformans* H99

and *C. gattii* WM161. Non-lytic exocytosis was more frequent in *C. neoformans* H99-infected cells than in *C. gattii*-infected cells.

Despite separation as a species 80 - 100 million years ago, the intracellular pathogenic strategy of *C. neoformans* and *C. gattii* was remarkably similar. Nevertheless, we observed quantitative differences between these strains, with more apoptotic cells present in Cg R265 and Cg WM179 - infected cells. We hypothesized that most of these apoptotic cells exhibit a "leaky" phagolysosomal membrane which is characterized by a LysoTracker negative population which could be correlated to faster *C. gattii* intracellular proliferation than *C. neoformans*, possibly causing physical damage to the membrane. Conservation of intracellular strategy among such temporally distant species implies that it is ancient and possibly maintained by extant selection pressures.

Acknowledgements

First and foremost, I would like to thank Dr. Arturo Casadevall for taking me into his laboratory. Dr. Casadevall has been a great mentor for me and has provided much support during my thesis work. My time at his laboratory has been a great experience.

Second, I would like to thank everyone in the Casadevall lab for being very supportive and collaborative. I would like to thank Radames Cordero and Anthony Bowen for their help on teaching me capsule and exo-polysaccharide isolation. I would like to thank Sarah Fu, Carlos De Leon Rodriguez, Eric Jung, and Diego Rossi for their help on cell culture work.

Lastly, I would like to thank my family for their continued love and support throughout my thesis work. My father has been a huge source of support and love all these years and without it, I would not be where I am today.

Table of Contents

List of Figures

Chapter 1: Introduction

History of *Cryptococcus* spp.

The first description of *Cryptococcus neoformans* as a human pathogen occurred 100 years ago. Abraham Buschke and Otto Busse at Griefswald University in Germany in 1894 isolated the fungus from the tibia of a 31-year-old woman with chronic tibial subperiosteal inflammation [1]. Busse believed that the organism was a *Saccharomyces*-like organism and thus termed the disease *saccharomycosis hominis.* Around the same time, Francesco Sanfelice at the University of Cagliari in Italy isolated an organism from fruit juices that he termed *Saccharomyces neoformans* that resembled Busse and Buschke's yeast [2]. Jean-Paul Vuillemin was the first to adopt the name '*Cryptococcus'* as the genus for both Busse-Buschke's yeast and Sanfelice's yeast [2,3]. Isolation of this fungus would continue, though the naming of it would remain inconsistent until 1950, when *Cryptococcus neoformans* was finally proposed as the species name by Rhoda Benham [2].

Since then, research on this organism has expanded and shed light on many of the major virulence factors that we are aware of today: the polysaccharide capsule and melanin, to name two [2]. Busse's early depictions of the yeast showed these organisms with an extremely thick cell wall that was also meticulously detailed by Ferdinand Curtis in 1896 [2]. Electron microscopy images of the fungus in 1976 by Mercedes Edwards and colleagues were some of the first images to capture the capsule, cell wall, plasma membrane, nucleus, nuclear membrane, and mitochondria of the organism and showed that the thickness of the capsule depends on the age of the cell [2]. Melanin production was first observed by Friedrich Staib in 1962 after the fungus was grown in media made from seeds of *Guizotia abyssinica*, though the pigment was not determined to be melanin until 1972 by Carol Shaw and L. Kapica of McGill University [2]. Despite these advances in understanding the pathogen, it

was not until the 1980's that *C. neoformans* was recognized as a major pathogen due to the emergence of the AIDS epidemic [4]. Since then, research has expanded our understanding of the virulence and pathogenesis of the organism.

Cryptococcus neoformans

Cryptococcus neoformans (Cn) is one of two etiological agents responsible for cryptococcosis and meningoencephalitis in HIV/AIDS patients [5,6]. Cn is an encapsulated basidiomycetous yeast that is ubiquitous in the environment, though it is predominately associated with avian excreta [5,7]. Within the species complex, there are two varieties, Cn var. *grubii* (Cng) and Cn var. *neoformans* (Cnn). Cng and Cnn are differentiated by serotype and molecular typing based on PCR fingerprinting, Amplified Fragment Length Polymorphism (AFLP) analysis, and Multilocus Sequence Typing (MLST) analysis [7]. Cng is of serotype A and molecular types VNI and VNII. Cnn is of serotype D and molecular type VNIV. Hybrids between the two varieties have been documented and are of serotype AD and molecular type VNIII [7]. Other molecular types have also been discovered more recently that do not fall into the four molecular type groups. These include a VNB molecular type that is consistently isolated from Botswana and other nearby African countries and a VNIc group that, unlike most of the VNI strains, was recovered from Asian patients that had cryptococcosis but were non-HIV patients [7]. The molecular types have a global distribution, with VNI strains being the most commonly isolated [7]. Asia, Africa, Europe, and Brazil have the greatest frequency of VNI isolates of 81%, 68%, 59%, and 71%, respectively [7]. However, the largest burden of the cryptococcosis is in the HIV/AIDS population of sub-Saharan Africa, where an estimated 625,000 deaths per year occur due

to cryptococcosis and cryptococcal meningitis [6]. Due the huge impact this disease has, and its global distribution, understanding Cn is of major import.

Cn is unique among most fungi in that, in addition to the cell wall, the fungus is surrounded by a polysaccharide capsule [8]. Although this capsule cannot be seen via regular microscopy techniques due to the highly hydrophilic nature of the capsule and high water content, it can be viewed using an India Ink stain [8]. The India Ink is not able to penetrate through the capsule, resulting in the distinctive white halo around the cell body of Cn [8]. The capsule is predominately composed of glucuronoxylomannan (GXM) and galactoxylomannan (GalXM), with GXM making up approximately 90% of the capsular polysaccharide [8]. Polysaccharide can also be shed extracellularly by the fungus and can be isolated using various purification techniques [8]. A large number of monoclonal antibodies (mAb) have been developed against various epitopes of GXM, underscoring the inherent immunogenicity of GXM [9,10]. This further supports the importance of the polysaccharide capsule of Cn, which is critical for virulence, as acapsular mutants do not cause disease in a murine model [8].

A typical infection with Cn is initiated by the inhalation of spores or desiccated yeast from the environment (Figure 1) [11]. While both spores and desiccated yeast have been proposed as the infectious propagule, evidence has shown that it is likely the spore that is the true contagious agent [12]. In addition, it has been shown that lethal brain infections can develop due to a spore inoculum alone, further suggesting a role for spores as the infectious agent [13,14]. Depending on the immune status of the host (i.e., immunocompromised or immunocompetent), the yeast either survives and proliferates within alveolar macrophages or remains in a latent stage within the macrophage, eventually forming cryptococcal

granulomas (cryptococcomas) [5]. Upon immunosuppression or reactivation, the yeast can then disseminate through the bloodstream to other organs, most often the central nervous system (CNS), where the yeast can cause fatal swelling of the meninges if left untreated [15]. Although disease may only develop in immunocompromised individuals, infection likely occurs in early childhood in most people, as antibodies to Cn can be detected in 70% of children older than 5 years and can be detected as early as 2 years of age [16].

Since the immune response is an important factor in determining whether infection with Cn progresses to clinical disease (namely meningoencephalitis), understanding this process is extremely important. An intact adaptive immune response with $CD4^+$ T helper cells type 1 (Th1) is critical for clearance of the pathogen, while a $CD4^+$ Th2 immune response has been shown to enhance fungal survival [17,18]. This explains the severe disease that results in HIV/AIDS and other immunocompromised patients infected with Cn. In addition to a Th1 response being critical for the clearance of the pathogen, a Th17 immune response has also been shown to play a role in the clearance of the pathogen [19]. An antibody response is also important for the clearance of Cn [20]. Anti-cryptococcal antibodies play a major role in enhancing phagocytosis and the Th1 response, making antibodies necessary for clearance [17]. IgM is important for preventing cryptococcosis, as mice lacking IgM had a much higher mortality and an increased fungal burden in the brain [17]. IgA may also play a role in the lung airways as it is abundant and plays roles in clearing viruses and bacteria in there; however, no evidence has been found to support this speculation [18].

Just as important as the adaptive immune response to *Cryptococcus* is the innate immune response, which is the first line of defense against this opportunistic pathogen. Alveolar macrophages are the major phagocytic innate cells that initially encounter this

pathogen in the lung [21]. Neutrophil infiltration into the lung also occurs early in the course of infection and the cells remain present throughout the course of a 28 day infection [21]. Interestingly, Cn infection is predominately intracellular, although extracellular yeast are present at 24 and 48 hours post-infection; however, by 28-days, the yeast are almost exclusively phagocytosed by macrophages [21]. Cn has been found to reside within the extremely acidic environment of the phagolysosome [21–23]. Unlike other pathogens that reside within the phagolysosome, Cn does not actively regulate the pH of the acidic compartment [22]. However, Cn does regulate the expression of host proteins that are important for maturation of the phagolysosome, namely Rab5 and Rab11, two GTPases on the membrane of phagosomes [24]. An interesting phenomenon that has been reported to occur in macrophages infected with Cn is extrusion from the phagosome [25]. This phenomenon has been termed non-lytic exocytosis (NLE) and three types have been characterized: partial, complete, and cell-to-cell transfer [26]. It has been shown that NLE is dependent on the pH of the phagolysosome, as drugs that modify the pH affect the frequency of non-lytic exocytosis in infected macrophages [27]. The mechanism of this phenomenon and why it occurs, however, has yet to be established. It is believed that phagosomal extrusion of Cn is one of the mechanisms responsible for fungal dissemination into the brain via macrophages [25–27].

Cryptococcus gattii

Like Cn, *C. gattii* (Cg) is also a basidiomycetous yeast. However, the two species likely diverged 80 - 100 million years ago which roughly corresponds to the separation of South America and Africa [28]. Cg can be divided into four molecular groups based on AFLP

analysis: VGI, VGIIa/b, VGIII, and VGIV [7,29]. The global distribution of Cg is nowhere near as widespread as Cn, and was originally thought to be restricted to the tropics and subtropics, especially Australia, where it is endemic [7,29]. However, the outbreak in Canada and the Pacific Northwestern USA from 1999 to 2007 has challenged this established view [30–32]. This outbreak was due to VGIIa/b molecular types and resulted in an incidence of Cg infections much greater than where Cg infection is endemic in Australia at a rate of 0.94 cases per million residents [7,30,33]. Within the Pacific Northwest United States, a novel VGIIc molecular type was also identified that was only documented in the US [34]. During the outbreak, incidence of the infection ranged from 8.5 to 37 cases per million residents [30]. Most patients infected with Cg were immunocompetent individuals, which differed from the typical Cn infection involving immunocompromised patients. Although the outbreak has ended, recent reports indicate that the pathogen is now endemic in the Vancouver Islands [35].

The emergence of this pathogen in temperate climates and its ability to infect both immunocompromised and immunocompetent hosts has resulted in an expansion of research into the pathogen. Many of the studies aim to understand the differences between Cn and Cg. One of the major differences between these two pathogens is the strength of the immune response induced in patients. The Cg outbreak strain (R265) at 7 days post infection induces lower levels of protective inflammatory cytokines TNFα, MCP-1, and IL-6 as compared to Cn H99 strain [36]. It was also shown that the Th1 immune response, which is critical for clearance of *Cryptococcus sp.*, is reduced in Cg-infected mice, as the Th1 cytokine IL-12 was found to be extremely low [36]. Lower levels of Th1 and Th17 cells were also found to be present in Cg-infected mice with both outbreak and non-outbreak

strains [37]. Pulmonary cytokine transcripts of *Ifng* were also expressed at lower levels in Cg-infected mice [37]. Interestingly, expression of *Il13* transcripts, a Th2 cytokine, were greater in Cg-infected mice compared to Cn-infected mice [37]. Further, decrements of Th1/Th17 responses are associated with poor activation of dendritic cells (DC), which express lower levels of MHC class II on their surface [37]. This poor activation is likely due to the ability of Cg to prevent DC maturation due to capsule composition and to its ability to induce a less potent inflammatory response [38,39].

Like Cn, the capsule of Cg is a major virulence factor [40]. Similar to the Cn capsule, the capsule of Cg is composed of glucuronoxylomannan (GXM), galactoxylomannan (GalXM), and various mannoproteins [40]. It has been shown that while the major components of the cryptococcal capsule are similar, differences do exist in the acetylation of the capsule [39]. The xylose content of the capsule of Cg is slightly greater than Cn and based on structural analysis, there is one less O-acetylation group present on the capsule of Cg strain JP02, a VGIIa hypervirulent strain isolated from patients in Japan [39].

Although they may share the same set of core virulence factors (capsule, melanin, urease, growth at 37°C, phospholipase), slight differences exist, such as the capsule composition mentioned previously. There are even traits that are only important for virulence in Cg but not for Cn, such as a lack of RNA interference machinery in the Vancouver Island outbreak strains and a deubiquinase that has different effects in Cn and Cg [41,42]. It is thought the lack of RNAi machinery may actually be protective against organisms that take advantage of it [40]. Deletion of the deubiquinase gene (*Ubp5*) in Cg resulted in hypermelanization and capsule growth, a phenotype that was opposite of that exhibited by Cn [42]. Interestingly, the deletion of this gene leads to Cg being more resistant

to oxidative and NO stress, while at the same time being susceptible to cell wall damage, which is different from that of Cn [42].

Another interesting difference between Cg and Cn is a 'division of labor' phenotype present in intracellular infections [43]. Unlike Cn, intracellular proliferation rates (IPR) of Cg cells within macrophages is much greater and has been shown to correlate with increased virulence, as the outbreak strains exhibited greater IPR than the non-outbreak Cg strains [44]. In these outbreak strains with increased IPR, no know virulence factors were associated with this trait, however, mitochondrial genes were found to be upregulated 10-fold, suggesting the importance of mitochondrial function in virulence [44]. Furthermore, Cg outbreak strains were found to have unique mitochondrial morphology that was not present in non-outbreak strains. A tubular morphology was observed in these outbreak strains that likely has a protective role in facilitating intracellular growth due to increased mitochondrial fusion events and occurred rapidly following internalization [43,44]. Although tubular morphology of the mitochondria has been observed in Cn, it has not been shown to predict virulence [45]. It was also shown that this morphology was present in not all the intracellular fungi, and that fungi that exhibited a tubular morphology were extremely resistant and non-proliferative, which possibly suggests some fitness benefit at the population level [43].

These distinct differences in the intracellular life of Cg and Cn and the capsule suggest even more differences may exist. We therefore were interested in examining the intracellular life of Cg and in exploring additional differences in features of survival within macrophages as well as further characterizing the capsule of Cg.

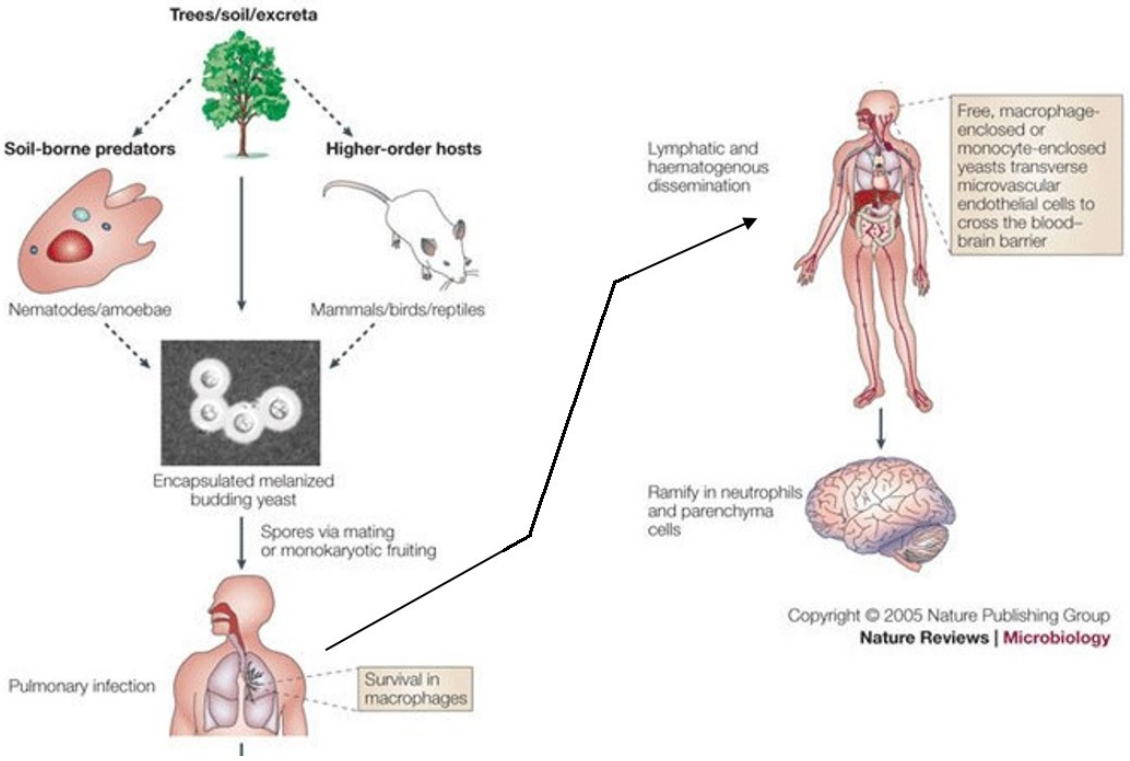

Figure 1: Disease progression of *Cryptococcus* infection. Infection results from inhalation of desiccated yeast or spores from the environment (trees/soil/avian excreta). The lung is the first organ infected in the host. If the host is immunocompetent, disease is cleared or granuloma forms. For an immunocompromised host, dissemination to other organ systems occurs, namely the CNS. Adapted from (11).

Chapter 2: Capsular and Exo-Polysaccharide of *Cryptococcus gattii*

The polysaccharide capsule of *Cryptococcus neoformans* (Cn) and *Cryptococcus gattii* (Cg) are a major virulence factor that has roles in inhibiting phagocytosis and immune suppression [46]. As mentioned previously, the capsule of Cg has been shown to have fewer of the O-acetylation groups on the GXM that are thought to contribute to inhibiting DC maturation and antigen presentation [38,39]. We sought to further characterize this virulence factor in *C. gattii*.

Methods

Fungal Strains: *Cryptococcus gattii* strain A1M R265 (ATCC# MYA-4093), *C. gattii* strain WM179 (ATCC# MYA-4560), *C. gattii* strain WM161 (ATCC# MYA-4562), and *Cryptococcus neoformans var. grubii* strain H99. Strains were stored at -80°C. Frozen stocks were streaked onto Sabouraud Dextrose Agar (SDB) (BD) and incubated at 30°C.

Polysaccharide Isolation: *Cryptococcus* strains were grown in Minimal Media (MM) (29.4 mM KH_2PO_4, 10 mM $MgSO_4 \cdot 7H_2O$, 13 mM Glycine, 3 μM Thiamine, @ pH 5.5) for 7 days. Cultures were then spun down at 4800*g*. For the first spin, the supernatant was collected, filtered through a 0.22 μm Stericup filter, and sequentially put through 100 kDa, 10 kDa, and 1 kDa filters (EMD Millipore). After each filtration, a gel formed on the membrane and this gel was collected and frozen at -20°C. The pellet from the first spin was washed 2 times with 1x PBS. A volume of DMSO (Sigma Aldrich) equal to the pellet was added and incubated at room temperature for 1 hour with regular shaking. The solution

was then spun down at 4800*g* and the supernatant was collected. Dialysis against deionized water to remove the DMSO from the polysaccharide was then performed on the supernatant and the dialyzed solution was frozen at -20°C. The frozen samples were then lyophilized, weighed, and suspended in MilliQ water at a concentration of 1 mg/ml.

Capsule size measurements: Cultures were grown in Minimal Media (MM) for 6 days and Difco's Sabouraud Dextrose Broth (SDB) (BD) for 48 hours. Cultures were washed three times with 1 X PBS and 3 µl of the pellet were transferred to microscope slide. An equal volume of India Ink was also added. Images were taken on an Olympus AX740 Microscope (Olympus) using a Retina QImaging camera. 100 cryptococci were analyzed per slide.

ELISA: The GXM capsular, 10 kDa, and 1 kDa fractions isolated from each strain were coated on a 96-well plate at a concentration of 1 µg/ml in 1X PBS and incubated at 4°C overnight. The plate was washed three times with TBST (2 M Tris base @ pH 7.2, 5 M NaCl, 1 M NaN_3, 0.1% TWEEN-20). Blocking solution (1% Bovine Serum Albumin and 0.1 M NaN_3 in 1x PBS) was added to the wells and incubated overnight at 4°C. Primary antibodies with specificity to glycan epitopes of Cn GXM (18B7, 12A1, 13F1, and 3E5) were added at a concentration of 10 µg/ml in Blocking Solution with a series dilution of 1:2 and incubated at 37°C for 1 hour. Goat-anti-mouse kappa chain antibodies conjugated to alkaline phosphatase were added at a 1:1000 dilution in Blocking Solution and washed three times with TBST. P-nitrophenyl phosphate in Substrate buffer (0.001 M $MgCl_26H_2O$ and 0.05 M Na_2CO_3) at a concentration of 1 mg/ml was added and the plate was developed

at 37°C for 30 minutes and absorbance was measured at 405 nm using the EMax Plus Microplate Reader (Molecular Devices).

Results

As the molecular structure of the capsule of Cg and Cn have already been shown to be different, we were interested in determining if the size of the capsule was different if the fungi was grown in different media. Difco's Sabouraud Dextrose Broth (SDB) is a nutrient rich medium that generally results in poor capsule growth. Between Cg R265 (the outbreak strain) and Cn H99, the radii of the capsule differed by 0.1432 μm, which was a statistically significant difference (Figure 2A). Statistically significant differences were observed among all strains. Interestingly, the capsule radius of Cg WM179 (a reference strain for VGI strains) was 3.704 μm on average (Figure 2A). This significantly larger capsule in Cg WM179 cultures was not expected, as SDB generally induces poor capsule growth. A recent study has shown that the capsule of VGI strains was larger than the other molecular types, which is consistent with our observation [47]. Capsule growth was significantly greater in Minimal Media (MM), yet Cg WM179 exhibited the same capsule radius when grown in SDB (Figure 2B). In SDB, the capsule radius of Cg WM179 was 3.704 μm while in MM the radius was 3.82 μm. In both SDB and MM, Cg WM179 had the largest capsule radius.

Since an antibody-mediated immune response is important for clearance of cryptococci, we sought to examine the binding of four monoclonal antibodies (mAb) that our laboratory has developed against the main component of the polysaccharide capsule of

Cn, GXM. As GXM can also be shed extracellularly, we were also interested in examining binding of the mAbs to the capsular glycans contained in 1 kDa and 10 kDa fractions (the 100 kDa fractions were not recovered due to technical complications) [8]. 18B7 is an IgG1 mAb that binds to an epitope of GXM in Cn H99 [10]. Binding of this antibody to the capsular polysaccharide (CPS) and exopolysaccharide (EPS) fractions of both Cn H99 and Cg R265 differed. At higher concentrations of 18B7, the mAb was less efficient at binding to CPS and EPS of Cg R265 as compared to Cn H99 (Figure 3). This trend was consistent with the binding of the other three anti-GXM monoclonal antibodies (Figures 4, 5, and 6).

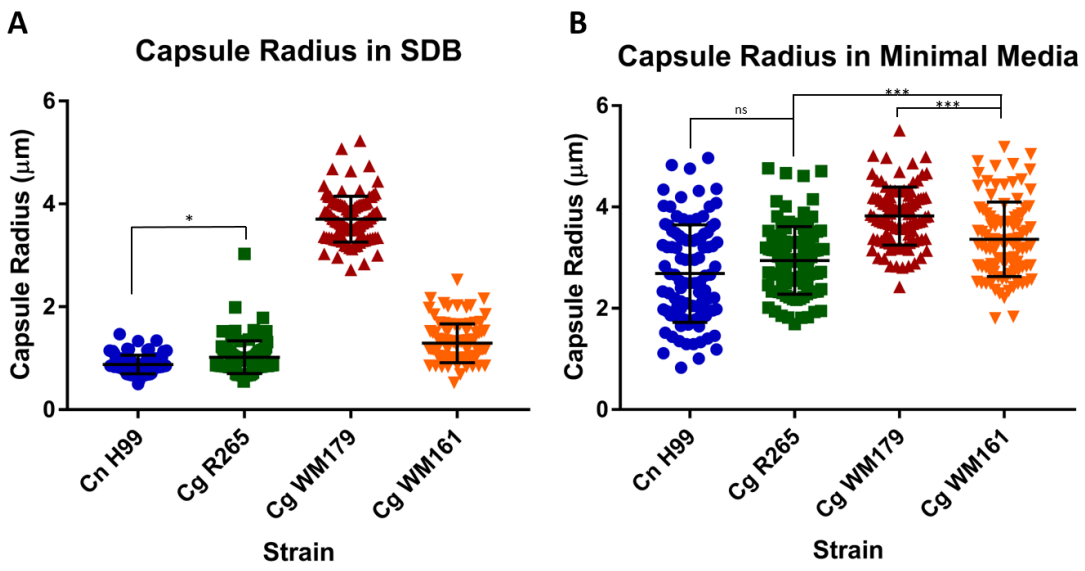

Figure 2: (A) Capsule Radius in Sabouraud Dextrose Broth (SDB) and (B) Capsule radius in Minimal Media (MM). Cultures in SDB were grown for 48 hours, washed with PBS, and pelleted, while cultures for MM were grown for approximately 6 days, washed, and pelleted. Both cultures arose from the same starter culture of SDB. Equal volumes of India Ink and a dense pellet mixture were added to glass slides. Each point on the graph represents the measurement of cryptococcal radius from one experiment. Unless noted otherwise, the P-value was less than 0.0001 (* = $P < 0.1$, *** = $P < 0.001$; all values determined using Tukey's test).

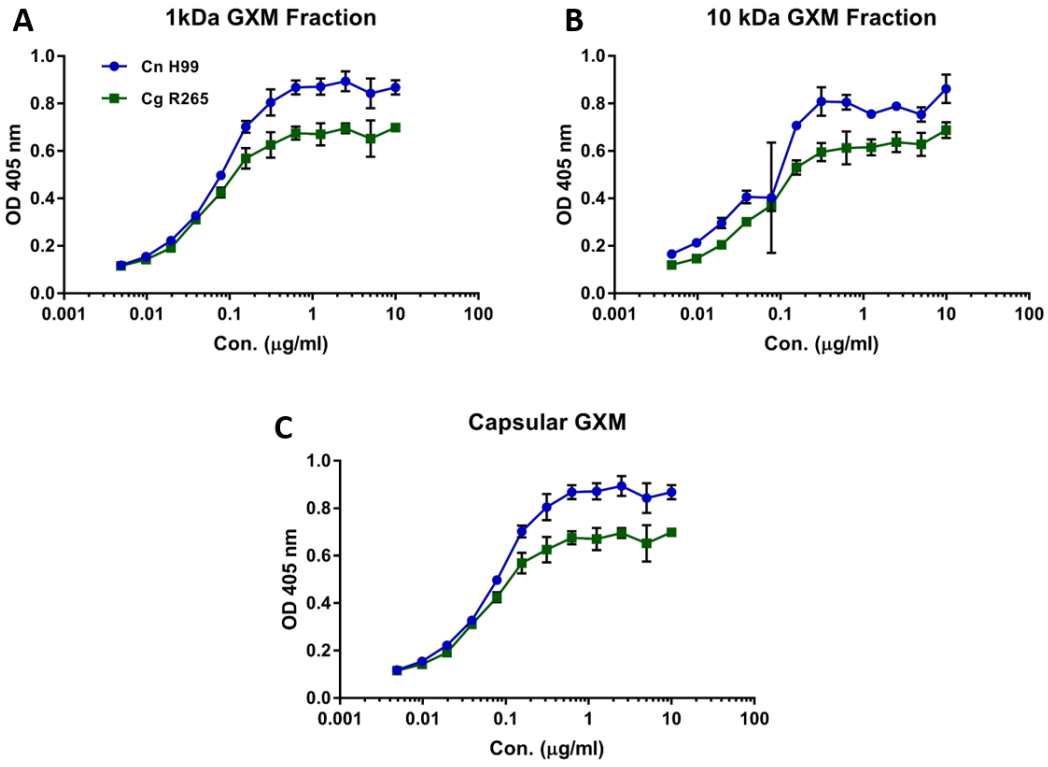

Figure 3: 18B7 binding to capsule polysaccharide (CPS) and 1 kDa and 10 kDa exopolysaccharide (EPS) fractions. (A-C) Binding was determined using an ELISA in which GXM fractions at 1 µg/ml in PBS coated the plate. 18B7 IgG1 monoclonal antibody (mAb) at a stock concentration of 10 µg/ml in Blocking Solution was serially diluted 1:2 approximately 11 times and the dilutions were added to the coated wells. Incubation conditions are outlined in Methods. Goat-anti-mouse kappa light chain conjugated to alkaline phosphatase was added after washing three times. The substrate, p-nitrophenyl phosphate, was added in substrate buffer at a concentration of 1 mg/ml. The plate was developed for 30 minutes at 37°C and read on an EMax Plus Microplate Reader at an absorbance of 405 nm. Data points represent the average of 4 wells on a single plate and error bars represent standard deviation.

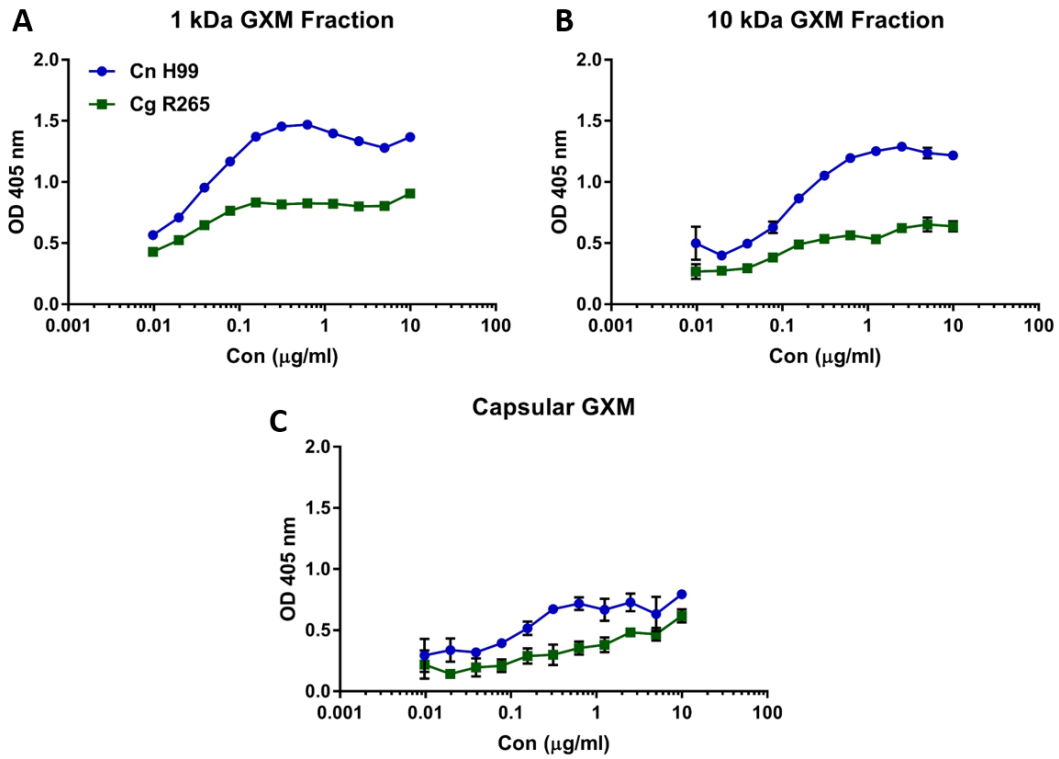

Figure 4: 3E5 binding to GXM fractions and capsular polysaccharide. Same ELISA set up as Figure 3, except with 3E5 IgG1.

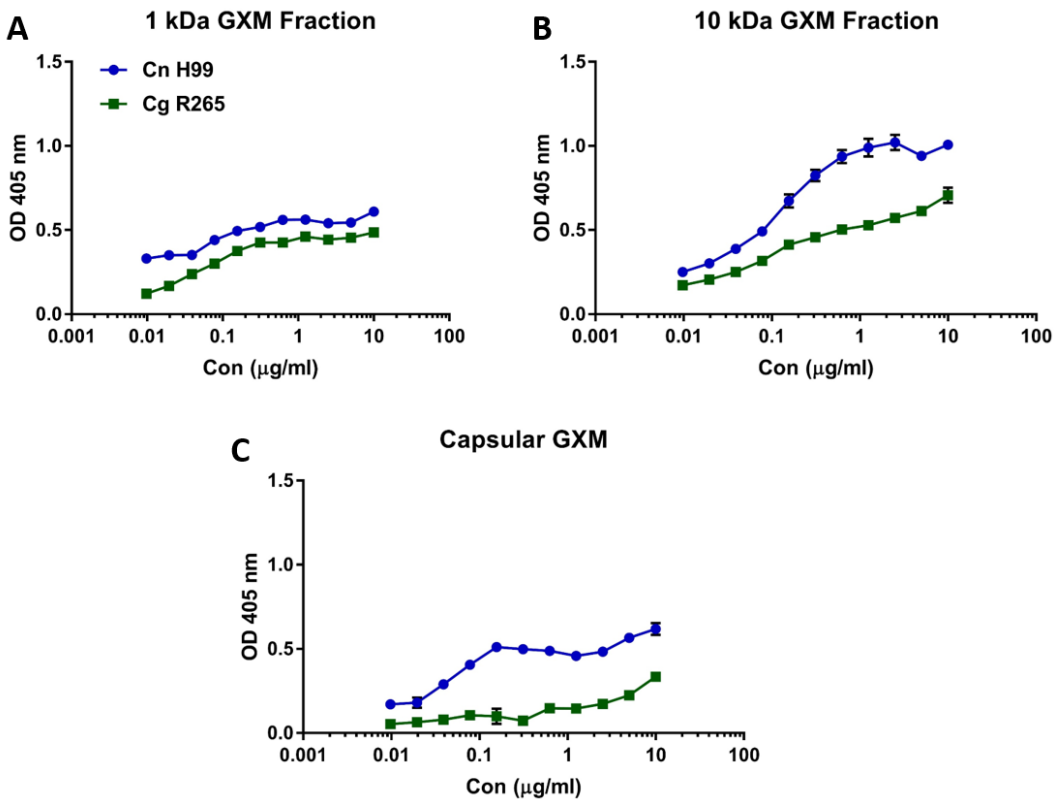

Figure 5: 12A1 binding to GXM Fractions and Capsule polysaccharide. Same ELISA set up as Figure 3, except with 12A1 IgM.

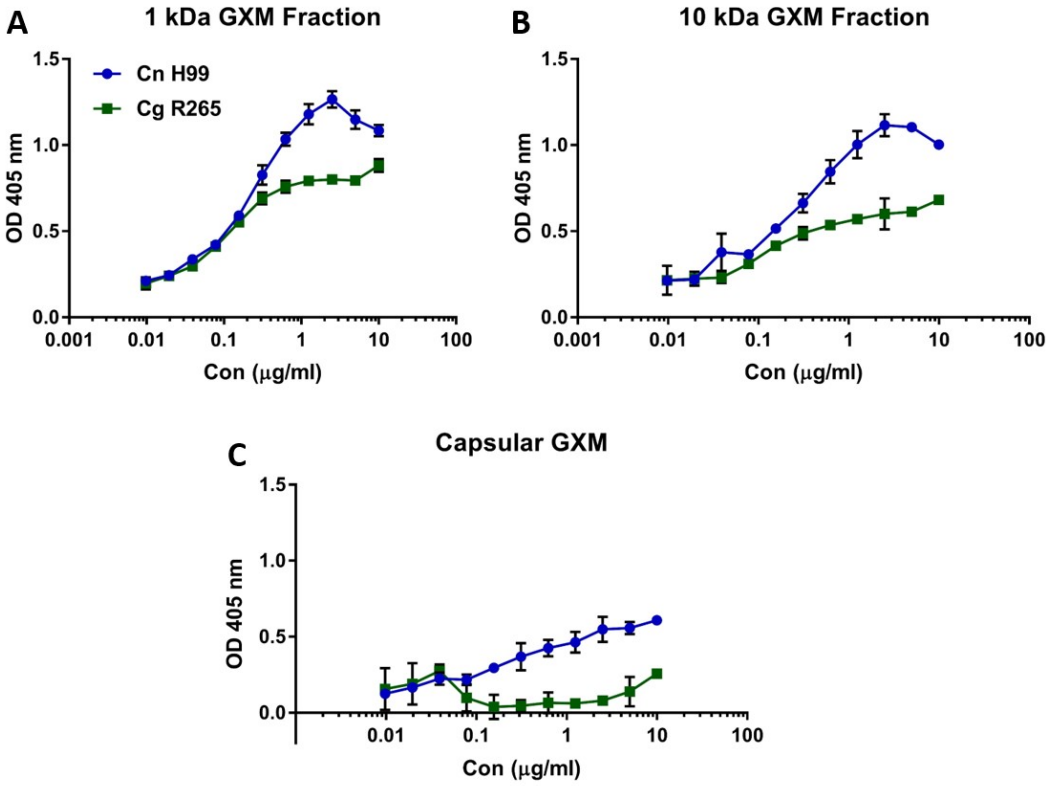

Figure 6: 13F1 binding to GXM fractions and capsule polysaccharide. Same ELISA set up as Figure 3, except with 13F1 IgM.

Chapter 3: Intracellular Pathogenic Strategy of *Cryptococcus gattii*

Intracellular survival of *Cryptococcus* species is a critical aspect of virulence and disease pathogenesis. Although much has been characterized in Cn, questions remain and even more questions are outstanding for Cg. A high intracellular proliferation rate has been associated with increased virulence in outbreak-associated Cg strains, a phenotype not observed for Cn strains [43]. This suggests a difference in the intracellular strategy that could provide further insights into the differential pathogenesis of the two fungal pathogens. We thus sought to identify and investigate these potential differences.

Methods

Mice: For all experiments, C57B/6 female mice 6 – 8 weeks of age were used and were obtained from Jackson Laboratory.

Cell Lines: Primary macrophages were obtained via bone marrow isolation from C57B/6 mice. The skin of each leg was peeled back and muscle cut away to reveal the bone. Once the skin and muscle were removed, the tibia and femur were removed and placed in DMEM Feeding media (20% L929 supernatant, 10% FBS, 0.1% β-mercaptoethanol, 1% Pen/Strep, 1% MEM-NEA Non-essential Amino Acids, 1% Glutamax, 1% HEPES Buffer). Marrow was then flushed out with Feeding Media, filtered through 0.22 μm filter, and centrifuged at 1200 rpm for 5 minutes at 4°C. Supernatant was discarded and the pellet was suspended in 20 ml of Feeding Media. Re-suspended solution was seeded onto 100 mm tissue culture-treated Petri dishes (Corning) and incubated at 37°C for 6 days. J774.16 murine

macrophage-like cells from frozen stocks were plated onto 6-well plates containing DMEM Complete Media (10% FBS, 10% Medium NCTC-109, 1% Pen/Strep, 1% MEM NEA Non-essential Amino Acids).

Phagocytosis Frequency: Approximately 5 x 10^4 BMDM were seeded onto the wells of a 24-well plate containing DMEM Feeding Media. BMDM were incubated overnight at 37°C with IFN-γ and LPS at a concentration of 0.5 μg/ml and 100 U/ml, respectively. Cryptococcal cultures for infection were opsonized with the 18B7 anti-GXM mAb at a concentration of 10 μg/ml for 5 minutes, left un-opsonized, or opsonized with 10% FBS in 1X PBS. BMDM were infected at an MOI of 3:1 (Cryptococci:BMDM). Infected BMDM were incubated at 37°C for 1.5 hours. Phagocytic frequency was determined by dividing the number of infected BMDM by the number of uninfected plus infected BMDM.

Measurement of Phagolysosomal pH: Approximately 1.25 x 10^5 BMDM were seeded onto wells of a 24-well tissue culture plate containing 12mm coverslips and DMEM Feeding Media. Macrophages were incubated at 37°C and activated overnight with LPS and IFN-γ at 0.5 μg/mL and 100 U/mL, respectively. Macrophages were infected at an MOI of 3:1 (about 3.75x10^5 fungal cells/well) with cryptococcal strains opsonized with mAb 18B7 conjugated to Oregon-Green at a concentration of 10μg/ml (Molecular Probes). The plate was spun down immediately at 1200 rpm for 1 minute to facilitate contact with the monolayer. The Oregon-Green fluorescent dye is pH sensitive at an excitation of 488 nm and insensitive at an excitation of 440 nm [48]. Infected macrophages were then incubated at 37°C for 10 minutes to initialize phagocytosis. For each strain of the two *Cryptococcus*

spp., a standard curve was generated to determine the pH at various time points after phagocytosis was initiated. For the standard curve, wells were incubated and washed with the desired pH calibration buffer for 5 minutes at 37°C. Nigicerin (5 mg/mL) was added at a final concentration of 5 μg/mL to equilibrate the buffer. The 12 mm coverslips were then removed and placed in culture side down on a 35 mm culture dish (MatTek) and images were obtained on the FITC channel (440nm and 488nm) using a QImaging Retiga 1300 camera attached to an Olympus AX70 Microscope. For the samples, coverslips were placed in HBSS media and imaged on the Olympus AX70 Microscope (Olympus). Imaging was done through the MetaFluor Fluorescence Ratio Imaging Software (Molecular Devices) for Olympus. Analysis of images was also performed on the MetaFluor Software.

pH Calibration Buffers: Calibration buffers were made for pH 3.0 to pH 7.0, at increments of 0.5 units. Buffers were composed of 140mM KCl, 1mM $MgCl_2$, 1mM $CaCl_2$, and 5 mM Glucose. For solutions with a pH less than 5.0, acetic acid was added to the mixture to adjust the pH. For solutions with a pH between 5.5 and 6.5, 2-ethanesulfonic acid (MES) was used. For pH greater than 7.0, HEPES was used as the buffer. The pH was then adjusted to desired values using either 1M KOH or 1M HCl.

Measurement of Membrane Permeabilization and Apoptosis: J774.16 macrophage-like cells or BMDM were seeded into a 6-well plate at 1 x 10^6 cells per 2 mL of media (DMEM Complete Media for J774.16 cells or DMEM Feeding Media for BMDM) and activated overnight with LPS and INF-γ (0.5 μg/mL and 100U/mL, respectively). The following day, cells were infected with cryptococci stained with Uvitex 2B (which binds to the cell wall

of fungi) at an MOI of 1:2 for a period of 24 hours. Cultures were opsonized with the mAb 18B7 at a concentration of 10μg/ml. One hour before the incubation period, LyosTracker Deep Red was added to each sample well and the single stain control. Once the 24-hour incubation period was finished, supernatant was collected and transferred to a corresponding 15 ml Falcon tube. Each well was washed with 1X HBSS and HBSS was collected and transferred to the corresponding Falcon tube. After the wash, 1 ml of Cellstripper (Corning) was added to each well and incubated at 37°C for 5 minutes. Cells were then collected and centrifuged for 5 minutes at 1200 rpm. After centrifugation, supernatant was discarded and the pellet was suspended in 1X HBSS and stained with CD11b-PE (clone M1/70) (eBioscience) and incubated for 5 minutes followed by centrifugation for 5 minutes at 1200 rpm. Supernatant was discarded and the pellet was suspended in 1X HBSS and transferred to FACS tubes and placed on ice. F2N12S and SYTOX-PE-Cy5.5 AADvanced Dead Cell Stain (Thermofisher Scientific) was added 5 minutes before analysis with Becton Dickinson LSRII flow cytometer (BD Biosciences).

Measurement of Non-Lytic Exocytosis: BMDM were seeded at $5x10^4$ cells onto 35 mm culture dishes (MatTek) containing DMEM Feeding Media and incubated at 37°C for 2 hours to induce adherence to the plate. Macrophages were then activated using LPS and IFN-γ at a concentration of 0.5 μg/mL and 100 U/mL, respectively. A *Cryptococcus* culture was prepared and the mAb 18B7 was added to the culture at a concentration of 10 μg/ml to enhance phagocytosis. The *Cryptococcus* strains were added at an MOI of 3:1 (approximately $1.5x10^5$ cells). The infected macrophages were then incubated at 37°C. Time-lapse images were taken every 4 minutes for a period of 24 hours at 37°C with 10%

CO_2 at 10x magnification on the Axiovert 200M Microscope (Zeiss). Time-lapse movies were analyzed using the Axio Vision Software (Zeiss) and number of cells exhibiting non-lytic exocytosis was recorded.

Urease Activity Measurement: *Cryptococcus* cultures were grown in SDB for 17 hours. Cultures were washed, counted, and diluted to a concentration of approximately 1.11 x 10^7 cells/ml. Approximately 1 x 10^6 cells were added onto a 96 well-plate. To measure activity, the Urease Activity Assay (Cat. # MAK120) from Sigma Aldrich was used and their protocol was followed. Briefly, an ammonium standard is prepared that was at a concentration of 500 µM. Then, 90 µl of the sample or the ammonium standard were added to the wells of a 96-well plate. 10 µl of urea was added and the plate was incubated for 2 hours at 30°C. Reagent A was added to stop the urease reaction. Then Reagent B was added to develop the plate and incubated at room temperature for 30 minutes. The plate was then read on the EMax Plus Microplate Reader (Molecular Devices) at a wavelength of 650 nm. Activity was determined by the following equation: $Urease\ Activity = \frac{(A_{sample} - A_{blank}) * n}{t * s}$, where n was the dilution factor, t was the incubation time in minutes, and s was the slope of the standard curve.

Nitric Oxide Measurement: Approximately 1.5 x 10^4 BMDM were seeded onto the wells of a 96-well plate containing DMEM Feeding Media. Cells were activated overnight with IFN-γ and LPS at a concentration of 100 U/ml and 0.5 µg/ml respectively, IFN-γ only at a concentration of 100 U/ml, or left inactivated. After BMDM cells were infected at an MOI of 1:1 for 48 hours, supernatants were collected. To determine NO_2- concentration, the

Griess reaction was performed. Supernatant (50 µl) was added to the wells of a 96-well plate and 50 µl of the Griess Reagent was added (a 1:1 mixture of 0.1% naphthylethylenediamine dihydrochloride and 1% sulfanilamide in 5% H_3PO_4) and incubated at room temperature for 30 minutes. Absorbance at 570 nm was recorded using the EMax Plus Microplate Reader (Molecular Devices).

Results:

We were first interested in directly comparing the efficiency of phagocytosis of Cn and Cg, as the capsule structure has been shown to be different enough to potentially affect binding of antibody and influence the activation complement [39]. The frequency of phagocytosis was greatest for all strains when opsonized with mAb 18B7, a monoclonal antibody against the GXM of Cn. Complement-treated *Cryptococcus* had a significantly lower frequency of phagocytosis for all strains and was very similar to the no-antibody control. Phagocytic frequency was essentially similar among all strains tested, contrary to our hypothesis. Cg WM161 had a phagocytic frequency of 83%, Cn H99 had a frequency of 81%, and Cg R265 had a frequency of 73% (Figure 7). For complement-treated *Cryptococcus*, phagocytic frequency was the same among all strains and not statistically different from the corresponding non-opsonized controls (Figure 7).

Once Cn and Cg are phagocytosed by cells, they reside in the phagolysosome [21,22]. It is known that Cn has the ability to modulate the phagolysosome by affecting the expression of the Rab GTPases on the surface of the phagolysosome [24]. Cn resides within

the phagolysosome at pH values between 4 and 5. Modulation of the pH of the phagolysosome via chemical drugs has a role in affecting non-lytic exocytosis [27].

Thus, we were interested in examining the potential differences of pH of the phagolysosomal compartments where Cn and Cg reside. We hypothesized that the phagolysosomal pH (ppH) would be affected differently in the macrophages. However, we saw that this was not the case. Phagolysosomal pH (ppH) in BMDM was measured at 0, 1, 2, 3, 4, and 24 hours post infection (Figure 8 A-F). At 0 hours, the mean ppH was highest for both Cg R265 and Cg WM179 strains, with Cg WM179 having the most basic ppH of 5.6 and Cg R265 having a ppH of 5.3 (Figure 8A) (p value <0.0001). The ppH of both Cg strains dropped after the 1 hour post-infection and did not return to baseline levels (Figure 8G). Interestingly, the ppH of Cn H99 was highest at 4 hours post infection, which was the opposite trend of the Cg strains. At 0 hour, Cn H99-infected BMDM had the lowest ppH of 5.2, as compared to the Cg-infected BMDM (Figure 8A). The ppH of Cn H99 was relatively consistent at 1 and 2 hours post infection, each being approximately 5.2 (Figure 8B and 8C). We also measured the pH of phagolysosomes at 24 hours in apoptotic and live BMDM infected with Cn H99 and Cg R265 (Figure 8F). Average ppH in apoptotic BMDM was greater than live infected BMDM. Phagolysosomal pH was 0.14 units greater in Cn H99-infected apoptotic BMDM compared to Cg R265-infected apoptotic BMDM (Figure 8F). Live Cn H99-infected BMDM had a ppH that was 0.52 units greater than the ppH of live Cg R265-infected BMDM. Phagolysosomal pH increased from 4 to 24 hours in both Cn H99-infected BMDM and Cg R265-infected BMDM, and was the highest at 24 hours (Figure 8G).

The distribution of points at each time interval among the strains also varied significantly. At time 0 hour, Cn H99-infected cells had the widest distribution of ppH values, ranging from 4.4 to 7.2. At 1 hour post infection, Cg R265-infected cells had the widest distribution, ranging from 2.0 to 5.8. Cn H99-infected cells had ranges from 4.5 to 5.9, while Cg WM179-infected cells ranged from 4.6 to 5.9. At 2 hours post infection, Cg R265-infected cells had the greatest distribution of ppH values, ranging from 4.2 to 5.9. At 3 hours post infection, Cn H99-infected cells had the widest distribution of ppH values ranging from 4.4 to 6.0. At 4 hours post infection, the ppH of Cg R265-infected cells had the widest distribution of ppH values ranging from 3.5 to 5.9. Finally, at 24 hours post infection a wide range of ppH was also observed, from a ppH of 1.5 to a ppH of 6.7.

We next sought to examine differences in phagolysosome membrane permeabilization in live, dead, and apoptotic populations over a 24-hour period. We first performed experiments in J774.16 murine macrophage-like cells and found that cells infected with Cg R265 or Cg WM179 had a larger population of apoptotic cells than cells infected with Cn H99 (46.32% and 50.55% versus 26.77%, respectively) (Figure 9E). Cg WM161– infected J774.16 cells had the largest population of live cells, at 60.83%, followed by Cn H99 which was 56.95%. Both Cg R265 and Cg WM179-infected cells had low percentages of live cells of 42.83% and 38.93%, respectively. Cg R265 infected J774.16 had 4.347% dead cells, which was the lowest number of dead cells among all strains, while Cn H99-infected cells had the highest of 13.91% (Figure 9E).

BMDM cells were infected with *Cryptococcus spp.* to verify the findings in J774.16 cells. Different results were obtained in infected BMDM cells as live and dead populations of *Cryptococcus*-infected BMDM were much greater than apoptotic populations, which

was not observed in infected J774.16 cells (Figure 10E). Cg WM179-infected BMDM had 10.38% more apoptotic cells than Cn H99-infected BMDM and 8.59% more apoptotic cells than Cg R265-infected BMDM. Cn H99-infected BMDM had the lowest number of apoptotic cells, which was 2.423% while Cg WM179-infected cells had the highest of 12.8%.

Lysosomal membrane damage has been associated with Cn virulence within the macrophage [49]. We sought to examine differences between Cn and Cg-infected macrophages. Based on the absence of LysoTracker Deep Red and presence of Uvitex 2B fluorescence, we could determine the number of infected cells that had undergone phagolysosomal membrane permeabilization (PMP), suggesting that *Cryptococcus* is the cause of the PMP. Both Cg R265 and WM179-infected J774 cells had the greatest numbers of cells exhibiting PMP, which were 698.4 and 1756.8, respectively (Figure 9N). Cg WM179 – infected J774 cells had 1058.4 more cells with PMP compared to Cg R265 – infected J774 cells, however this difference was not statistically significant. Cg R265 infection resulted in 496.3 more cells as compared to Cn H99 infected J774 that had PMP, yet this difference was also not statistically different. Cg R265-infected J774 had 96.2 more cells with PMP than Cg WM161-infected cells (Figure 9N). Cg WM179-infected cells had 1154.6 more cells with PMP as compared to Cg WM161-infected cells (Figure 9N). Cn H99-infected cells had 1554.7 fewer PMP events than Cg WM179-infected cells.

Apoptotic BMDM exhibited a similar pattern to J774 cells, in that Cg R265 and Cg WM179-infected cells had the greatest number of PMP events. Cg WM179-infected cells had 33.67 cells with PMP, which was 21 more than Cn H99 infected cells (Figure 10N).

The number of live cells infected with *Cryptococcus spp.* was very low and comparable to J774 cells (Figure 10N).

Non-lytic exocytosis (NLE) events have been reported in Cn-infected macrophages and has been hypothesized to assist in dissemination to the CNS via a Trojan Horse mechanism [50]. This phenomenon has not been as readily observed in Cg infected macrophages. Cg has been shown to be less neurotrophic than Cn strains[51]. Thus, we hypothesized that there would be a lower frequency of non-lytic exocytosis events associated with Cg infections. We found that Cn H99-infected cells had more of Type I, Type II, and Type III exocytosis events than all the Cg-infected cells (Figure 11A). We found that Type II (partial exocytosis) was more frequent in Cn H99, ranging from 2.34% to 4.8% more (Figure 11A). Cg WM179 and Cg WM161 infections were found to have no Type I (complete exocytosis) events. Cg R265-infected cells more often exhibited Type III (cell-to-cell transfer) events at a frequency of 3.15%, which was the greatest among Cg-infected cells. Cg WM179-infected cells had Type II events at a frequency of 4%, which was the greatest among Cg-infected cells (Figure 11A). Comparing overall NLE among all strains, Cn H99-infected cells exhibited NLE at a frequency of 14.75%, which was greater than all Cg-infected cells (Figure 11B). Cg R265-infected cells had a frequency of NLE of 7.29%, the largest among the Cg-infected cells. Cell lysis was greatest in Cg WM179-infected cells and was not found in Cg WM161-infected cells. Based on the above results, Cn H99-infected BMDM more frequently exhibit NLE than Cg-infected cells.

Urease is considered an important virulence factor in *Cryptococcus* infection and thought to have a potential role in affecting the pH of phagolysosomes [52]. Urease activity *ex vivo* was found to be relatively similar among the Cg strains, with Cg WM179 having

the highest activity *ex vivo* of 1.436 U/L (Figure 12). Cg R265 had the next highest activity of 1.42 U/L, followed by Cg WM161 which had an activity of 1.384 U/L. Cn H99 had the lowest activity of 1.215 U/L. No statistical significance was observed between the strains.

One of the antimicrobial defense mechanisms of innate immune cells such as macrophages is the production of reactive oxygen and reactive nitrogen species. It has been shown that Cn reduces the levels of nitric oxide produced by macrophages independent of iNOS [53]. However, the effect that Cg has on NO_2- production has not been shown. Following methods similar to that reported by Trajkovic et al. [53], we found that Cg WM161 affects production of nitric oxide the least, regardless of whether macrophages were untreated, treated with IFN-γ, or treated with IFN-γ and LPS. BMDM activated with IFN-γ only and infected with Cn H99 induced 0.77 μM of NO_2- while Cg WM161 induced 3.34 μM of nitric oxide (Figure 13). Interestingly, the uninfected control produced significantly larger concentration of nitric oxide, which was a concentration of 11.63 μM, which likely suggests that both Cn and Cg reduce NO_2- production in macrophages to varying degrees.

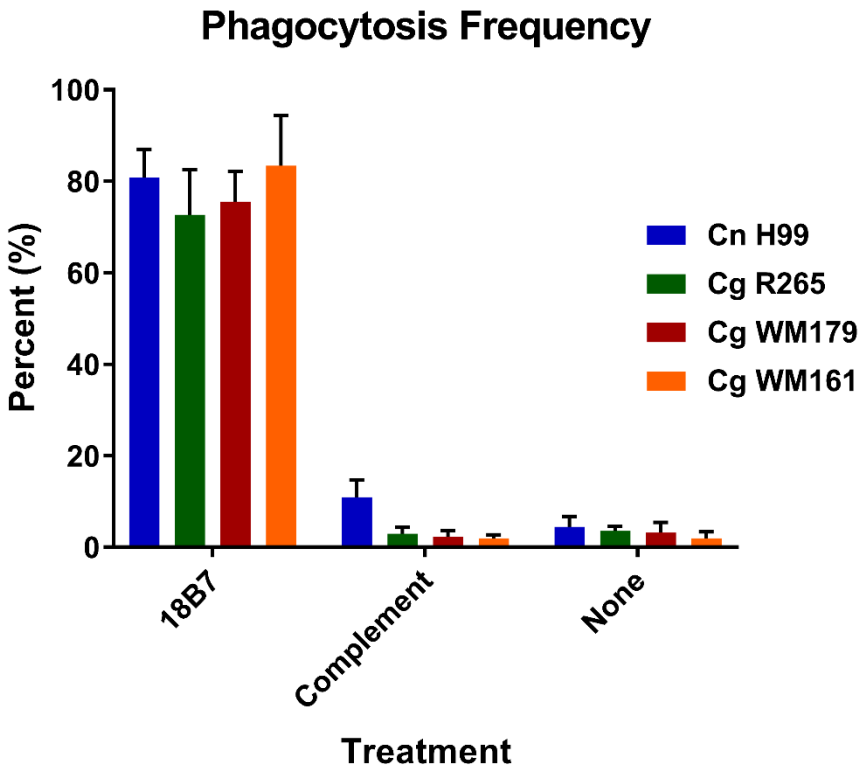

Figure 7: Phagocytosis frequency of *Cryptococcus* strains. Cultures were treated with mAb 18B7 or complement (10% FBS in DMEM Media). Untreated *Cryptococcus* cultures was used as a negative control. One experiment with triplicate wells for each strain was performed. No significant difference was observed among strains.

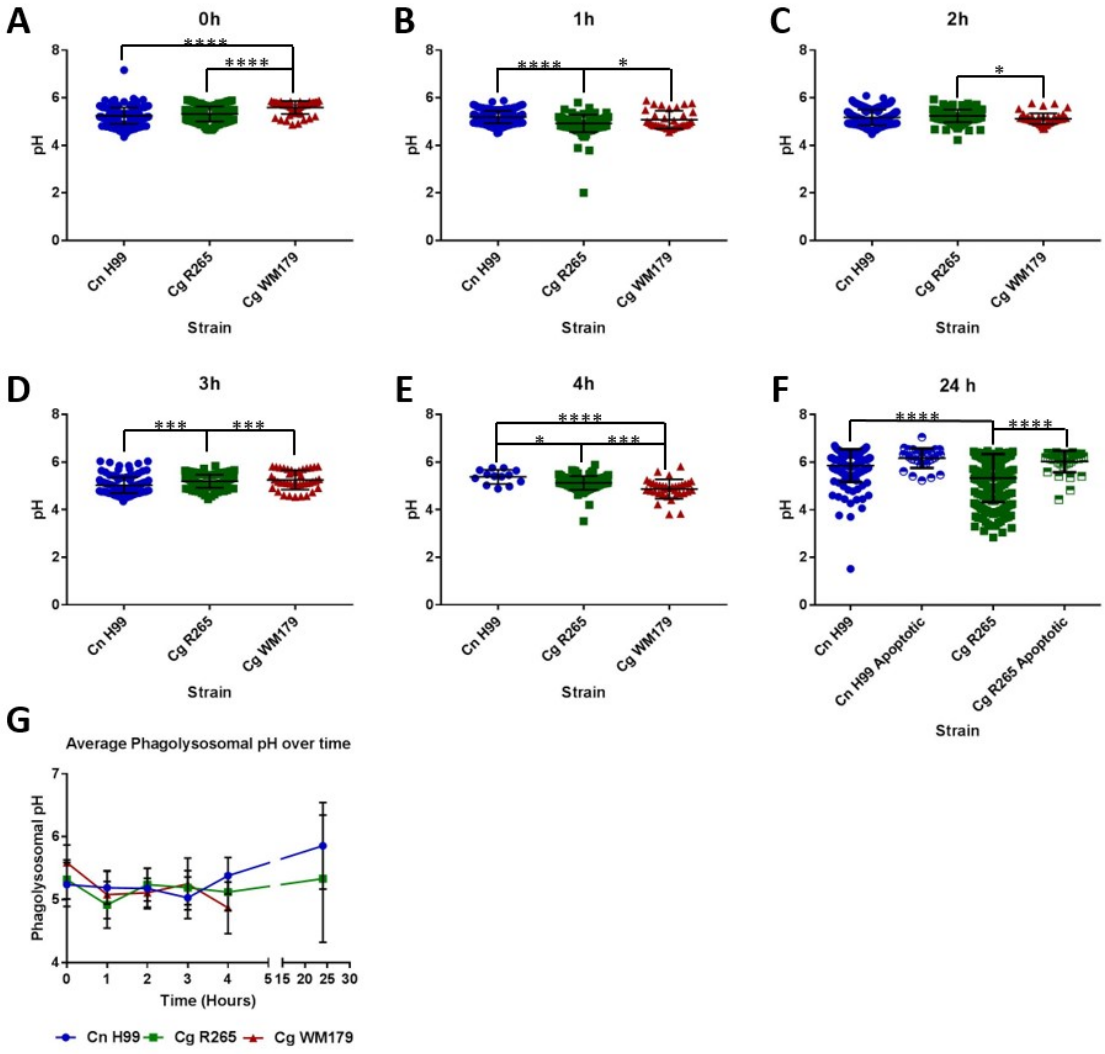

Figure 8: Phagolysosomal pH in infected BMDM. (A-E) Phagolsyosomal pH in BMDM infected with cryptococcal strains at 0 to 4 hours post-infection (p.i.) was determined using dual ratio fluorescent microscopy. The pH remained essentially the same over the time intervals within and among strains. Data points represent individual phagolysosomes (F) Phagolysosomal pH at 24 hours p.i. determined in apoptotic and live cells. Apoptotic populations were determined via the presence of Annexin V. (G) Average pH over 24-hour time interval. One experiment was performed for each time interval. P values were

determined using 2-way ANOVA and Tukey's test (**** = $p < 0.0001$, *** = $p < 0.001$, * = $p < 0.05$).

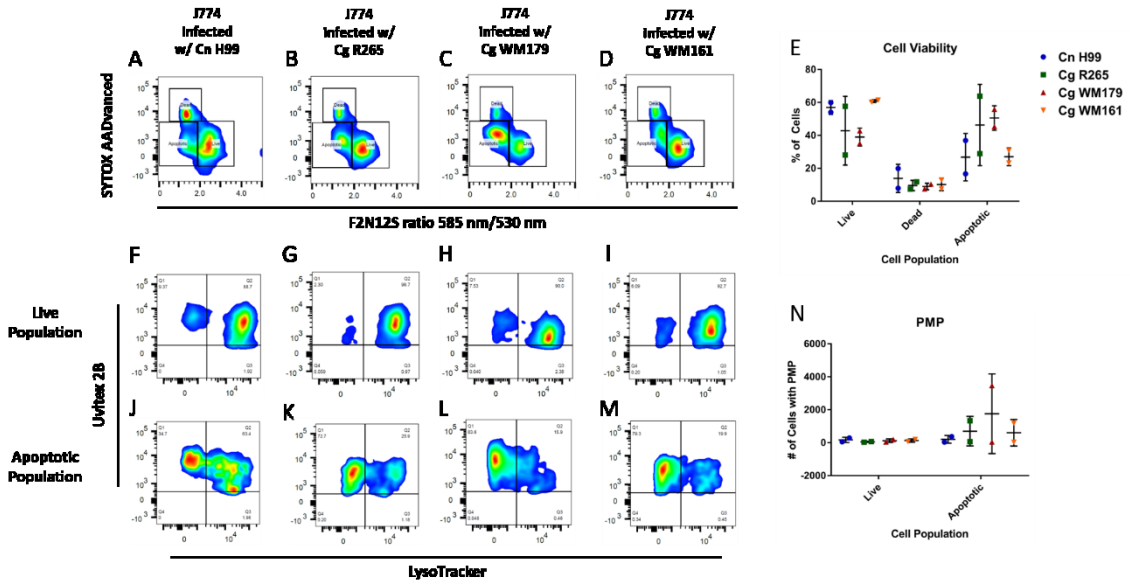

Figure 9: Cell viability and phagolysosomal membrane permeabilization (PMP) in J774 cells after 24 hours. (A-D) Representative population of infected J774 cells (Dead, Apoptotic, and Live) with *Cryptococcus spp.* Among two independent experiments performed, results were comparable. Each point represents the average of triplicate samples from one experiment. (E) Cell viability in J774 cells examining each population of cells. (F-M) Representative populations of J774 infected cells examining PMP for Live (F-I) and Apoptotic (J-M). Among two experiments, populations were comparable. (N) PMP in J774 cells infected with *Cryptococcus spp.* Data points represent average of triplicate samples of one experiment. Error bars represent standard deviation.

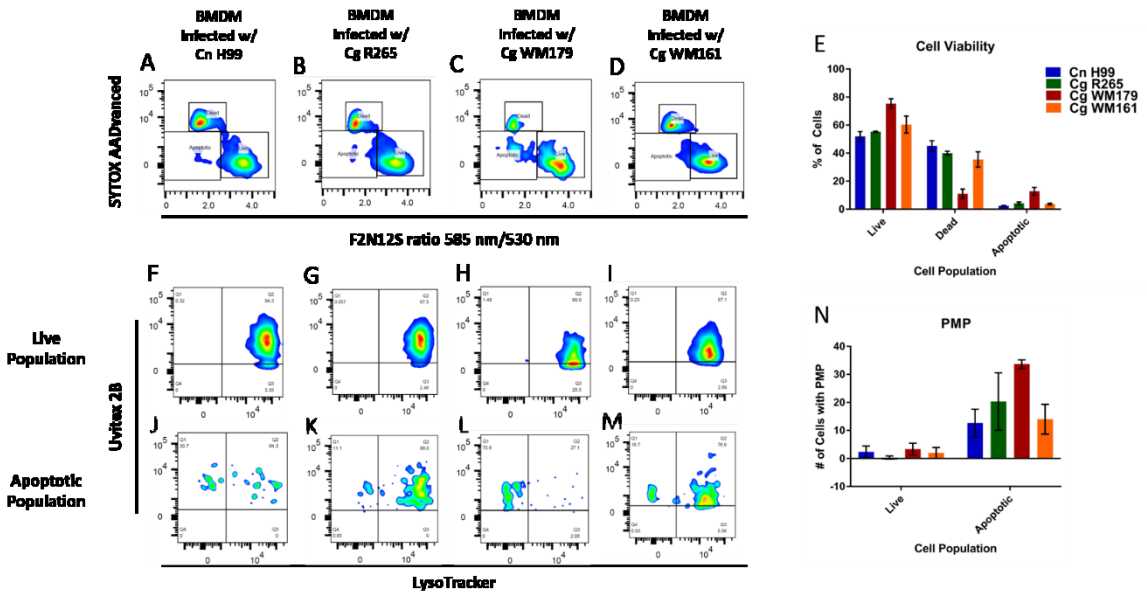

Figure 10: Cell viability and PMP in infected BMDM after 24 hours. (A-D) Representative population of cells (Dead, Live, and Apoptotic). (E) Cell viability of infected BMDM. Frequencies were based off averages of triplicate samples in one experiment. (F-M). Representative population of infected BMDM to determine PMP in Live (F-I) and Apoptotic (J-M) populations. Populations are representative of triplicate samples in one experiment. (N) PMP in live and apoptotic populations of BMDM infected with *Cryptococcus spp*. Data represents average of triplicate samples in one experiment. Error bars represent standard deviation.

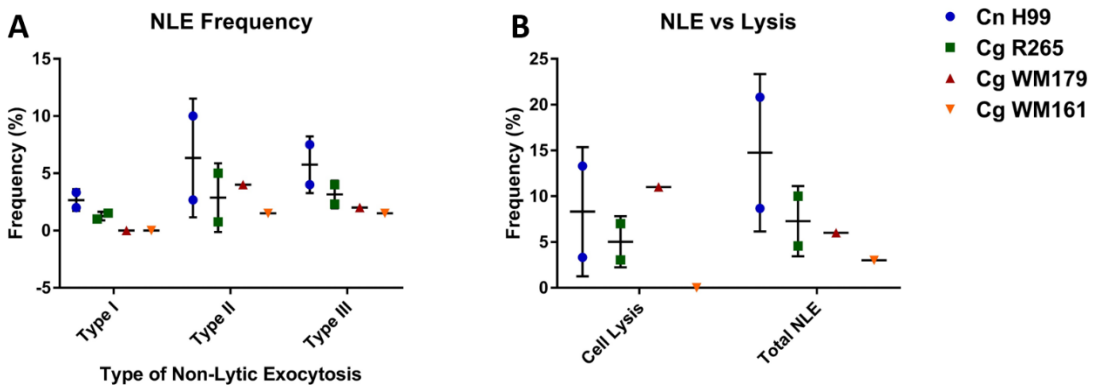

Figure 11: Frequency of non-lytic exocytosis (NLE) in BMDM over a 24-hour infection period. (A) Type I (Complete exocytosis), Type II (Partial exocytosis), and Type III (Cell-to-cell transfer) frequencies in BMDM infected with Cn H99, Cg R265, Cg WM179, and Cg WM161. Two independent experiments were carried out for Cn H99, Cg Wm179, and Cg WM16l and three for Cg R265. (B) Total frequency of NLE in infected BMDM compared to cell lysis. No statistical difference was found (Tukey's test).

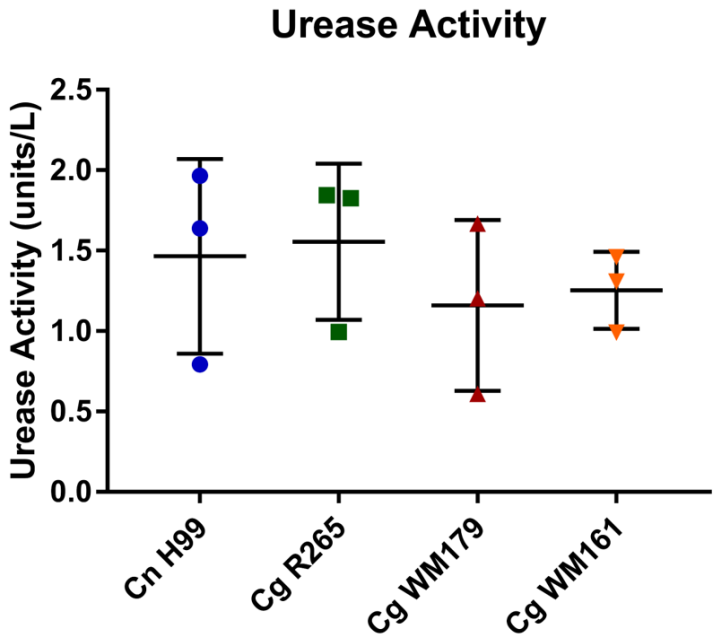

Figure 12: Urease activity *ex vivo* after following two hours of incubation with urea. Activity was determined using the Urease Activity Assay (Sigma-Aldrich). Three independent experiments with four replicate wells per strain were performed. Error bars represent standard deviation. No significant difference was found (Tukey's Test).

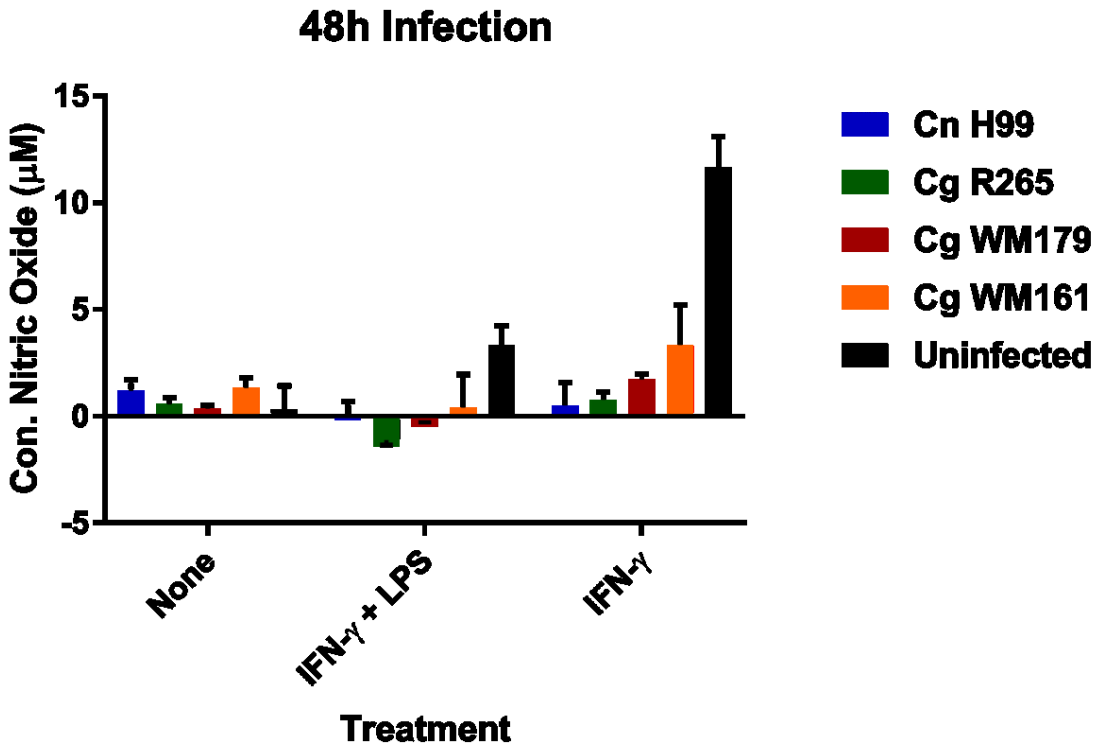

Figure 13: Production of nitric oxide after 48 hours infection. BMDM were infected with *Cryptococcus* cultures for 48 hours and supernatant was collected. Griess Reaction was performed to determine NO_2- production. Triplicate wells were carried out for each strain and error bars represent standard deviation.

Chapter 4: Discussion and Conclusions

Cryptococcus neoformans and *Cryptococcus gattii* are two fungal species separated by approximately 80 - 100 million years of evolution, roughly correlating with the separation of Africa and South America [28]. It is likely that Africa and South America (specifically northern Brazil) are the likely origin of Cn and Cg, respectively [54–56]. However, despite their long period of separation and location of origin, they have not differed in their core virulence factors: capsule, melanin, urease, and ability to grow at 37°C [15,29].

Although these virulence factors are conserved in both species, there does appear to be quantitative differences between Cg and Cn. It has been shown extensively that Cg induces a less protective immune response in immunocompetent hosts. This has been associated with the capsule of Cg, which is different in composition and has been shown to prevent DC activation [38,39]. Our results on mAb binding to GXM fractions showed that the mAbs bind much more effectively to Cn H99 capsule and GXM fractions than Cg R265 capsule and GXM fractions. This is further evidence that the composition of the capsules differ, as all four mAbs (18B7, 3E5, 12A1, and 13F1) bind to epitopes within the GXM of Cn [10]. Although the Cg strain examined by Urai et al. (JP02) was specific to Japan, the strain we used, Cg R265 was of the same molecular type, VGIIa [39]. Further, both strains were serotype B (ATCC), which suggests similar GXM composition. For future studies, examining the composition of Cg R265 capsular polysaccharide would enable us to make certain that the Japanese strain JP02 and Cg R265 are similar. It would be interesting to examine the biophysical properties of the *C. gattii* GXM. Biophysical properties of the *C. neoformans* capsule have been characterized, and as there are differences in the

composition of the polysaccharide, it is likely that several biophysical properties (zeta potential, dynamic light scattering, etc.) will differ between the species.

An interesting observation that was made while analyzing the capsule radii of Cg was that Cg WM179 (which is a VGI molecular type) had a much larger capsule than all the other strains grown in the medium SDB. SDB, which is a nutrient rich medium, is not used to induce capsular growth in Cn. The observation of such a large capsule was initially unexpected. However, our data is supported by the results and conclusions of a recent study that VGI strains have much larger capsules than the other molecular types [47]. It was also interesting to note that the capsule radius of Cg WM179 did not change much when grown in capsule-inducing media (Minimal Media). Cn H99 and the two other Cg strains did have a significant increase in capsule radius, which was expected. It is unclear why the capsule radius of Cg WM179 did not change, but it is possible that the mechanisms involved in the regulation of capsule synthesis differ in these organisms.

We were also interested in examining the intracellular survival strategy of Cg within macrophages. Mitochondrial regulation and intracellular proliferation are two unique traits of Cg that are important for virulence [43,44]. Understanding if other unique features responsible for increased virulence in Cg were of interest. Phagocytosis of both Cg and Cn requires opsonization by either complement or antibodies, as the capsule of both pathogens is inherently anti-phagocytic [18]. Based on our observation of reduced binding of the various mAbs to the GXM fractions of Cg R265 compared to Cn H99, we hypothesized that phagocytosis would occur at a lower frequency. However, we observed very little difference in the frequency of phagocytosis. Complement opsonized Cg and Cn resulted in nearly identical levels of phagocytic uptake as the un-opsonized controls, which was not

expected. This was likely due to using 10% FBS instead of freshly collected complement. Determining if the complement was indeed active could have insured that the C3 component would have been deposited on the cell wall of the fungus and lead to phagocytosis. It would also be interesting to examine phagocytosis frequency at early time points post-infection. Examining frequency at 0, 15, and 30 minutes post-infection could reveal distinct differences among the strains.

Following phagocytosis, Cn and Cg reside within the phagolysosome of macrophages [21,22]. We were interested in determining differences in the pH of phagolysosomes of infected BMDM over time. Contrary to our initial hypothesis, phagolysosomal pH remained relatively constant over time and among the strains from 0 to 4 hours post phagocytosis, though slight differences were detected. At 24 hours post-infection, more distinct differences were observed. Phagolysosomal pH was much greater in Cn-infected BMDM, regardless of whether these cells were live or apoptotic. Even though we observed more phagolysosomal membrane permeabilization in Cg-infected BMDM (and J774 cells), the difference in pH of the phagolysosomes at 24 hours did not fit with that observation. The expected observation was that the pH in the Cg-infected BMDM would be higher than Cn-infected BMDM, as a higher (or more basic) phagolysosomal pH has been associated with membrane damage [57]. It is possible that the difference in membrane damage was because Cg proliferates faster within the host cell than Cn, possibly leading to more damage. It has been hypothesized that phospholipase activity is likely responsible for inducing phagolysosomal membrane damage, and while we have not tested phospholipase activity for Cg and Cn, examining differences in activity *ex vivo* and *in vitro* could provide further insight into this observed difference.

As mentioned previously, Cn-infected macrophages can expunge the fungi, leaving both the macrophage and fungus intact [25]. This mechanism is believed to assist in dissemination of the organism to the CNS *in vivo* [27]. Compared to Cn, the frequency of NLE events occurred at a much lower frequency, which fits with the proposed purpose of the phenomenon; Cg VGIIa strains have been shown to establish disease in the lungs and rarely disseminate, while Cn strains predominately result in severe CNS disease [29,51]. If NLE acts to assist in dissemination, it follows that Cg R265 (and other outbreak strains) would have lower frequencies of the phenomenon. Further, it has been characterized through *in vitro* studies that Cn transmigration occurs at greater frequencies than Cg, which supports our results as well as the results of others [50].

Urease is important for hydrolyzing urea to produce ammonia and CO_2 and is found in many organisms, including bacteria and plants [52]. The presence of urease activity within microorganisms has been associated with virulence and increased pathogenesis [52]. Urease is an major virulence factor of Cn and is thought to play a role in survival within the phagolysosome and has been shown to have a role in aiding transmigration through the blood-brain barrier [52,58]. Examining urease activity *ex vivo* showed us that it is relatively the same among all strains examined. This result supports the notion that although the species separated tens of millions of years ago, a certain set of virulence factors have been maintained. To further understand urease activity during an infection, it will be necessary to infect macrophages and measure the urease activity of the strains after 24 hours. As urease activity is both important for intracellular survival and plays a role in transmigration, examining differences *in vitro* could provide further insight into differences observed in phagolysosomal pH and non-lytic exocytosis. While this is a relatively straightforward

approach, the assay that we used to measure urease activity is extremely sensitive. Slight changes in the culture age or incubation time result in very different results. To ensure that the *in vitro* assay works, making sure the same amount of *Cryptococcus* cells are used after the lysis of the macrophages is important.

Negative values were obtained from the nitric oxide assay, which is not biologically possible. It was possible that errors were made when preparing the Griess reagents, however, another member in our laboratory did get positive results. Likely, the preparation of our samples differed, though more experiments need to be performed to further optimize the assay. It is also possible that the conditions of our assay resulted in nitrite production below the threshold of detection.

Future Directions

Many of the observations on the pH and non-lytic exocytosis experiments were made using microscopy, yet flow cytometric assays have been used to examine the pH and non-lytic exocytosis over a 24 hour infection [27]. Carrying out these assays using Cg may reveal more information about the population of cells present and allow us to see if similar differences between microscopy and flow cytometry results arise.

One avenue of research that has not been explored in depth is the role of melanin during infection. It is known that melanin is an important virulence factor and has a role in preventing oxidative damage and cold damage, yet the exact role it has during infection is largely unknown [59]. Examining melanin expression between Cn and Cg would be the first step in determining if a difference even exists. Infecting BMDM with melanized and un-melanized strains would be a relatively straightforward process and seeing the effects on

pH, apoptosis, membrane damage, and non-lytic exocytosis would be insightful.

Lastly, examining the intracellular pathogenic strategy within amoeba would provide further insight into whether the minute differences observed in macrophages are indeed evolutionary conserved. Within the natural environment, the amoeba is a likely predator of *Cryptococcus spp*, and it has been suggested that the amoeba provided selection pressures to promote survival within mammalian macrophages [60]. Determining if similar results between Cg and Cn intracellular pathogenic strategy occur within amoebae would provide evidence that amoebae were a major driving force of selection pressures for intracellular survival.

Conclusions

In summary, while Cg and Cn diverged over 80 - 100 million years ago, their virulence factors remain relatively stable. Qualitative and quantitative differences in the virulence factors have been observed in the intracellular pathogenic strategies of Cn and Cg, yet the strategies are relatively conserved. Conservation of intracellular strategies among such temporally distant species implies that these evolved strategies are ancient and possibly maintained by common extant selection pressures.

References

1. Freij, J. B. & Freij, B. J. The earliest account of human cryptococcosis (Busse–Buschke Disease) in a woman with chronic osteomyelitis of the tibia. *Pediatr. Infect. Dis. J.* **34,** 1278 (2015).
2. Barnett, J. A. A history of research on yeasts 14:1 medical yeasts part 2, *Cryptococcus neoformans*. *Yeast* **27,** 875–904 (2010).
3. Srikanta, D., Santiago-Tirado, F. H. & Doering, T. L. *Cryptococcus neoformans*: historical curiosity to modern pathogen. *Yeast* **31,** 47–60 (2014).
4. Casadevall, A. & Perfect, J. R. *Cryptococcus neoformans*. *Cryptococcus neoformans* (American Society for Microbiology (ASM), 1998).
5. Mitchell, T. G. & Perfect, J. R. Cryptococcosis in the era of AIDS--100 years after the discovery of *Cryptococcus neoformans*. *Clin. Microbiol. Rev.* **8,** 515–48 (1995).
6. Park, B. J. *et al.* Estimation of the current global burden of cryptococcal meningitis among persons living with HIV/AIDS. *Aids* **23,** 525–30 (2009).
7. Cogliati, M. Global molecular epidemiology of *Cryptococcus neoformans* and *Cryptococcus gattii* : an atlas of the molecular types. *Scientifica (Cairo).* **2013,** 1–23 (2013).
8. Zaragoza, O. *et al.* in *Advances in Applied Microbiology* **2164,** 133–216 (2009).
9. Mukherjee, J., Nussbaum, G., Scharff, M. D. & Casadevall, A. Protective and nonprotective monoclonal antibodies to *Cryptococcus neoformans* originating from one B cell. *J. Exp. Med.* **181,** 405–9 (1995).
10. Feldmesser, M. & Casadevall, A. Mechanism of action of antibody to capsular

polysaccharide in *Cryptococcus neoformans* infection. *Front. Biosci* 136–151 (1998).

11. Idnurm, A. *et al.* Deciphering the model pathogenic fungus *Cryptococcus neoformans*. *Nat. Rev. Microbiol.* **3,** 753–764 (2005).

12. May, R. C., Stone, N. R. H., Wiesner, D. L., Bicanic, T. & Nielsen, K. *Cryptococcus*: from environmental saprophyte to global pathogen. *Nat. Rev. Microbiol.* **14,** 106–117 (2015).

13. Giles, S. S., Dagenais, T. R. T., Botts, M. R., Keller, N. P. & Hull, C. M. Elucidating the pathogenesis of spores from the human fungal pathogen *Cryptococcus neoformans*. *Infect. Immun.* **77,** 3491–3500 (2009).

14. Velagapudi, R., Hsueh, Y. P., Geunes-Boyer, S., Wright, J. R. & Heitman, J. Spores as infectious propagules of *Cryptococcus neoformans*. *Infect. Immun.* **77,** 4345–4355 (2009).

15. Kwon-chung, K. J. *et al. Cryptococcus neoformans* and *Cryptococcus gattii*, the etiologic agents of cryptococcosis. *Cold Spring Harb. Perspect. Med.* **4,** a019760 (2014).

16. Goldman, D. L. *et al.* Serologic evidence for C*ryptococcus neoformans* infection in early childhood. *Pediatrics* **107,** e66–e66 (2001).

17. Hole, C. & Wormley, F. L. Innate host defenses against *Cryptococcus neoformans*. *J. Microbiol.* **54,** 202–211 (2016).

18. Gibson, J. F. & Johnston, S. A. Immunity to *Cryptococcus neoformans* and *C. gattii* during cryptococcosis. *Fungal Genet. Biol.* **78,** 76–86 (2015).

19. Murdock, B. J., Huffnagle, G. B., Olszewski, M. A. & Osterholzer, J. J.

Interleukin-17A enhances host defense against cryptococcal lung infection through effects mediated by leukocyte recruitment, activation, and gamma interferon production. *Infect. Immun.* **82,** 937–948 (2014).

20. Casadevall, A. & Pirofski, L. -a. Antibody-mediated protection through cross-reactivity introduces a fungal heresy into immunological dogma. *Infect. Immun.* **75,** 5074–5078 (2007).

21. Feldmesser, M. *et al. Cryptococcus neoformans* is a facultative intracellular pathogen in murine pulmonary infection *Cryptococcus neoformans* is a facultative intracellular pathogen in murine pulmonary infection. *Society* **68,** 4225–4237 (2000).

22. Levitz, S. M. *et al. Cryptococcus neoformans* resides in an acidic phagolysosome of human macrophages. *Infect. Immun.* **67,** 885–890 (1999).

23. Wozniak, K. L. & Levitz, S. M. *Cryptococcus neoformans* enters the endolysosomal pathway of dendritic cells and is killed by lysosomal components. *Infect. Immun.* **76,** 4764–4771 (2008).

24. Smith, L. M., Dixon, E. F. & May, R. C. The fungal pathogen *Cryptococcus neoformans* manipulates macrophage phagosome maturation. *Cell. Microbiol.* **17,** 702–713 (2015).

25. Alvarez, M. & Casadevall, A. Phagosome extrusion and host-cell survival after *Cryptococcus neoformans* phagocytosis by macrophages. *Curr. Biol.* **16,** 2161–2165 (2006).

26. Stukes, S. A., Cohen, H. W. & Casadevall, A. Temporal kinetics and quantitative analysis of *Cryptococcus neoformans* nonlytic exocytosis. *Infect. Immun.* **82,**

2059–2067 (2014).

27. Nicola, A. M., Robertson, E. J., Albuquerque, P., Derengowski, L. d. S. & Casadevall, A. Nonlytic exocytosis of *Cryptococcus neoformans* from macrophages occurs i*n vivo* and is influenced by phagosomal pH. *MBio* **2,** e00167-11-e00167-11 (2011).

28. Sharpton, T. J., Neafsey, D. E., Galagan, J. E. & Taylor, J. W. Mechanisms of intron gain and loss in *Cryptococcus*. *Genome Biol.* **9,** R24 (2008).

29. Chen, S. C. A., Meyer, W. & Sorrell, T. C. *Cryptococcus gattii* infections. *Clin. Microbiol. Rev.* **27,** 980–1024 (2014).

30. Kidd, S. E. *et al.* A rare genotype of *Cryptococcus gattii* caused the cryptococcosis outbreak on Vancouver Island (British Columbia, Canada). *Proc. Natl. Acad. Sci. U. S. A.* **101,** 17258–17263 (2004).

31. MacDougall, L. *et al.* Spread of *Cryptococcus gattii* in British Columbia, Canada, and detection in the Pacific Northwest, USA. *Emerg. Infect. Dis.* **13,** 42–50 (2007).

32. Datta, K. *et al.* Spread of *Cryptococcus gattii* into Pacific Northwest Region of the United States. *Emerg. Infect. Dis.* **15,** 1185–1191 (2009).

33. Fraser, J. a *et al.* Same-sex mating and the origin of the Vancouver Island *Cryptococcus gattii* outbreak. *Nature* **437,** 1360–1364 (2005).

34. Byrnes Edmond J., I. J. *et al.* A diverse population of *Cryptococcus gattii* molecular type VGIII in Southern Californian HIV/AIDS patients. *PLoS Pathog.* **7,** (2011).

35. Espinel-Ingroff, A. & Kidd, S. E. Current trends in the prevalence of *Cryptococcus gattii* in the United States and Canada. *Infect. Drug Resist.* **8,** 89–97 (2015).

36. Cheng, P. Y., Sham, A. & Kronstad, J. W. *Cryptococcus gattii* isolates from the British Columbia cryptococcosis outbreak induce less protective inflammation in a murine model of infection than *Cryptococcus neoformans*. *Infect. Immun.* **77,** 4284–4294 (2009).

37. Angkasekwinai, P. *et al. Cryptococcus gattii* infection dampens Th1 and Th17 responses by attenuating dendritic cell function and pulmonary chemokine expression in the immunocompetent hosts. *Infect. Immun.* **82,** 3880–3890 (2014).

38. Huston, S. M. *et al. Cryptococcus gattii* capsule blocks surface recognition required for dendritic cell maturation independent of internalization and antigen processing. *J. Immunol.* **196,** 1259–71 (2016).

39. Urai, M. *et al.* Evasion of innate immune responses by the highly virulent *Cryptococcus gattii* by altering capsule glucuronoxylomannan structure. *Front. Cell. Infect. Microbiol.* **5,** 101 (2016).

40. Bielska, E. & May, R. C. What makes *Cryptococcus gattii* a pathogen? *FEMS Yeast Res.* **16,** fov106 (2016).

41. D'Souza, C. A. *et al.* Genome variation in *Cryptococcus gattii*, an emerging pathogen of immunocompetent hosts. *MBio* **2,** e00342-10-e00342-10 (2011).

42. Meng, Y. *et al.* Deubiquitinase Ubp5 is required for the growth and pathogenicity of *Cryptococcus gattii*. *PLoS One* **11,** 1–16 (2016).

43. Voelz, K. *et al.* 'Division of labour' in response to host oxidative burst drives a fatal *Cryptococcus gattii* outbreak. *Nat. Commun.* **5,** 5194 (2014).

44. Ma, H. *et al.* The fatal fungal outbreak on Vancouver Island is characterized by enhanced intracellular parasitism driven by mitochondrial regulation. *Proc. Natl.*

Acad. Sci. U. S. A. **106,** 12980–12985 (2009).

45. Ma, H. & May, R. C. Mitochondria and the regulation of hypervirulence in the fatal fungal outbreak on Vancouver Island. *Virulence* **1,** 197–201 (2010).

46. McClelland, E. E., Bernhardt, P. & Casadevall, A. Estimating the relative contributions of virulence factors for pathogenic microbes. *Infect. Immun.* **74,** 1500–1504 (2006).

47. Fernandes, K. E., Dwyer, C., Campbell, L. T. & Carter, D. A. Species in the *Cryptococcus gattii* complex differ in capsule and cell size following growth under capsule-inducing conditions. *mSphere* **1,** 1–13 (2016).

48. Canton, J. & Grinstein, S. in *Phagocytosis and Phagosomes: Methods and Protocols* (ed. Botelho, R.) **1519,** 185–199 (2017).

49. Davis, M. J. *et al. Cryptococcus neoformans*– induced macrophage lysosome damage crucially contributes to fungal virulence. *J. Immunol.* **194,** 2219–2231 (2015).

50. Sorrell, T. C. *et al.* Cryptococcal transmigration across a model brain blood-barrier: evidence of the Trojan horse mechanism and differences between *Cryptococcus neoformans* var. *grubii* strain H99 and *Cryptococcus gattii* strain R265. *Microbes Infect.* **18,** 57–67 (2016).

51. Ngamskulrungroj, P., Chang, Y., Sionov, E. & Kwon-Chung, K. J. The primary target organ of *Cryptococcus gattii* is different from that of *Cryptococcus neoformans* in a murine model. *MBio* **3,** e00103-12-e00103-12 (2012).

52. Feder, V. *et al. Cryptococcus gattii* urease as a virulence factor and the relevance of enzymatic activity in cryptococcosis pathogenesis. *FEBS J.* **282,** 1406–1418

(2015).

53. Trajkovic, V. *et al. Cryptococcus neoformans* neutralizes macrophage and astrocyte derived nitric oxide without interfering with inducible nitric oxide synthase induction or catalytic activity - possible involvement of nitric oxide consumption. *Scand. J. Immunol.* **51,** 384–391 (2000).

54. Hagen, F. *et al.* Ancient dispersal of the human fungal pathogen *Cryptococcus gattii* from the Amazon Rainforest. *PLoS One* **8,** e71148 (2013).

55. Souto, A. C. P. *et al.* Population genetic analysis reveals a high genetic diversity in the Brazilian *Cryptococcus gattii* VGII population and shifts the global origin from the Amazon Rainforest to the semi-arid desert in the northeast of Brazil. *PLoS Negl. Trop. Dis.* **10,** e0004885 (2016).

56. Litvintseva, A. P. & Mitchell, T. G. Population genetic analyses reveal the African origin and strain variation of *Cryptococcus neoformans* var. *grubii*. *PLoS Pathog.* **8,** e1002495 (2012).

57. Tucker, S. C. & Casadevall, A. Replication of *Cryptococcus neoformans* in macrophages is accompanied by phagosomal permeabilization and accumulation of vesicles containing polysaccharide in the cytoplasm. *Proc. Natl. Acad. Sci.* **99,** 3165–3170 (2002).

58. Shi, M. *et al.* Real-time imaging of trapping and urease- dependent transmigration of *Cryptococcus neoformans* in mouse brain. *J. Clin. Invest.* **120,** 1683–1693 (2010).

59. Almeida, F., Wolf, J. M. & Casadevall, A. Virulence-associated enzymes of *Cryptococcus neoformans*. *Eukaryot. Cell* **14,** 1173–1185 (2015).

60. Derengowski, L. da S. *et al.* The transcriptional response of *Cryptococcus neoformans* to ingestion by *Acanthamoeba castellanii* and macrophages provides insights into the evolutionary adaptation to the mammalian host. *Eukaryot. Cell* **12,** 761–774 (2013).

Joudeh Bishara Freij
Date of Birth: March 4, 1992
Place of Birth: Moscow, Russia
Cell Phone: 248-884-3067
Permanent Address: 1872 West Bend Drive, Bloomfield Hills, MI, 48302
Personal E-mail: jbfreij@gmail.com

Education

Johns Hopkins Bloomberg School of Public Health - Baltimore, MD *August 2015 to May 2017*

- Degree: Master of Science
- Total Credit Hours: 176
- Cumulative GPA: 3.85

University of Michigan - Ann Arbor, MI *2010-2014*

- Degree: Bachelor of Science
- Concentration: Microbiology
- Total Credit Hours Earned: 145
- Cumulative GPA: 3.469
- Sophomore – Senior GPA: 3.645

Oakland University – Rochester, MI *Summer 2012*

- GPA: 3.96
- Total Credits earned: 10

Academic Degrees

ScM	Johns Hopkins School of Public Health (expected May 23, 2017)
B.S.	University of Michigan, May 3, 2014

Research Experience

Dr. Arturo Casadevall's Laboratory, JHSPH, MD *January 2016 to Present*

- Studying the intracellular pathogenic strategy of *Cryptococcus gattii* in macrophages
- Completed ScM thesis in Dr. Casadevall's laboratory
- Have published Opinion piece on *C. gattii* and *C. neoformans* species separation
- Further improved cell culture and microscopy techniques
- Learned and performed Flow Cytometry to analyze membrane damage in infected macrophages
- Learned how to isolate melanin and capsular polysaccharide from cryptococcal cultures

Dr. Michal Olszewski's Laboratory, Ann Arbor VA Hospital, MI Fall Term 2012 to Summer 2014

- Studied *Cryptococcus neoformans* infection in mice and their immune responses
- Have been acknowledged in two publications from our laboratory
- Co-authored a research paper published by this laboratory
- Worked on understanding macrophage polarization in *C. neoformans* infection
- Experimental techniques I am proficient in include quantitative PCR, reverse transcriptase PCR, mRNA isolation, mice dissection, tissue culture, bone marrow macrophage isolation, culturing *C. neoformans*, hemocytometer counting, dilution plating
- Other experimental techniques I have learned include splenocyte culture, Griess reaction, microscopy, and ELISA
- Learned how to prepare various media and agars
- Studied the effect that *C. neoformans* has on lysosome damage and the possible mechanisms behind the damage

Research Scholars – U. of M. *Fall Term 2011 to Winter Tern 2012*

- Worked in Dr. Michal Olszewski Laboratory (Department of Pulmonary and Critical Care)
- Studied *Cryptococcus neoformans* infection in mice and their immune responses
- Further enhanced research techniques
- Learned several new techniques, such as ELISA, mRNA isolation, and quantitative PCR
- Presented research poster at the Research Scholar's Symposium
- Received Outstanding Poster Award for both the presentation of the project and the design of the poster

Undergraduate Research Opportunities Program – U. of M. Fall Term 2010-Winter Term 2011

- Worked in Dr. Dan Michele's Laboratory (Department of Molecular and Integrative Physiology)
- Worked on understanding proteins (dysferlin and syntaxin-4) thought to be involved in membrane repair
- Learned skills in cloning techniques, imaging analysis, microscopy, slide preparation, Western Blot, and PCR

Professional Society Memberships

American Society for Microbiology, Student Member *2014 - Present*

Awards/Honors

$500 Travel Award from the Medical Mycological Society of the Americas funded by Immuno-Mycologics, Inc., ASM Microbe 2017, New Orleans, LA, June 1-5. [Awarded to graduate students with the top four ranked abstracts in medical mycology at ASM Microbe 2017]

Publications in Peer-reviewed Journals

Davis MJ, Tsang TM, Qiu Y, Dayrit JK, **Freij JB**, Huffnagle GB, Olszewski MA. 2013. Macrophage M1/M2 polarization dynamically adapts to changes in cytokine microenvironments in *Cryptococcus neoformans* infection. *mBio* 4(3): e00264-13. Doi:10.1128/mBio.00264-13

Freij JB and Freij BJ. 2015. The earliest account of human cryptococcosis (Busse-Buschke disease) in a woman with chronic osteomyelitis of the tibia. *The Pediatric Infectious Disease Journal* 34(11): 1278

Dalmazi G, Hirshberg J, Lyle D, **Freij JB,** and Caturegli P. 2016. Reactive oxygen species in organ-specific autoimmunity. *Autoimmune Highlights* 7(11): 1-11. Doi: 10.1007/s13317-016-0083-0

Casadevall A, **Freij JB**, Hann-Soden C, Taylor J. 2017. Continental drift and speciation of the *Cryptococcus neoformans* and *Cryptococcus gattii* species complexes. *mSphere*. (in press)

Published Abstracts

Freij JB, Freij BJ. 2014. Abraham Buschke (1868-1943): A polymath's contributions to mycology, venereology, and dermatology [abstract number W-1449]. 114th General Meeting of the American Society for Microbiology, May 17-20, 2014.

Davis MJ, Eastman A, Qui YF, Malachowski AN, Hadd ZD, **Freij JB**, Carolan J, Potchen N, Olszewski MA. 2014. *Cryptococcus neoformans*-induced Iysosomal damage promotes intracellular survival and growth of the organism within macrophages. *Mycoses.* 57 (Suppl. 1); 25.

Freij BJ and **Freij JB**. 2016. "Sir Almost Right": the prodigious but colorful career of Sir Almroth Wright (1861 – 1947) [abstract number SUN-813]. ASM Microbe 2016 Abstracts, Boston, MA, June 16 – June 20, 2016.

Freij JB, Freij BJ. 2017. Lady Amalia Fleming: Physician, Bacteriologist, Greek Resistance Activist, and Politician. To be presented at ASM Microbe 2017, New Orleans, LA, June 1-5, 2017.

Freij JB, Rodriguez CDL, Fu M, Rossi DCP, Casadevall A. 2017. The intracellular pathogenic strategy of *Cryptococcus gattii* in macrophages. To be presented at ASM Microbe 2017, New Orleans, LA, June 1-5, 2017.

Presentations

Freij JB, McDade JR, Michele D. Molecular mechanisms of muscular dystrophy. *Undergraduate Research Opportunities Program Symposium,* University of Michigan, April 2011

Freij JB, Davis MJ, Dayrit JK, Olszewski MA. Macrophage polarization is plastic to changes in the cytokine environment during a *Cryptococcus neoformans* infection. *Research Scholars Symposium*, University of Michigan, April 2012.

Freij JB, Freij BJ. Abraham Buschke (1868-1943): A polymath's contributions to mycology, venereology, and dermatology. Presented 114th General Meeting of the American Society for Microbiology, Boston, MA, May 19, 2014.

Davis MJ, Eastman A, Qui YF, Malachowski AN, Hadd ZD, **Freij JB**, Carolan J, Potchen N, Olszewski MA. *Cryptococcus neoformans*-induced Iysosomal damage promotes intracellular survival and growth of the organism within macrophages. Presented at the 9th International Conference on *Cryptococcus* and Cryptococcosis, Amsterdam, The Netherlands, May 15-19, 2014.

Freij BJ, **Freij JB**. 2016. "Sir Almost Right": the prodigious but colorful career of Sir Almroth Wright (1861-1947). Presented at ASM Microbe 2016, Boston, MA, June 16 – June 20, 2016.

Freij JB, Freij BJ. 2017. Lady Amalia Fleming: Physician, Bacteriologist, Greek Resistance Activist, and Politician. Accepted for presentation at ASM Microbe 2017, New Orleans, LA, June 1-5, 2017.

Freij JB, Rodriguez CDL, Fu M, Rossi DCP, Casadevall A. 2017. The intracellular pathogenic strategy of *Cryptococcus gattii* in macrophages. Accepted for presentation at ASM Microbe 2017, New Orleans, LA, June 1-5, 2017.

Acknowledged for Technical Assistance for the Following Publications:

Davis MJ, Eastman AJ, Qiu Y, Gregorka B, Kozel TR, Osterholzer JJ, Olszewski MA. (2015). Cryptococcus neoformans–induced macrophage lysosome damage crucially contributes to fungal virulence. *The Journal of Immunology*, *194*(5), 2219-2231.

Qiu Y, Davis MJ, Dayrit JK, Hadd Z, Meister DL, *et al*. (2012) Immune modulation mediated by cryptococcal laccase promotes pulmonary growth and brain dissemination of virulent *Cryptococcus neoformans* in mice. *PLoS ONE* 7(10): e47853. doi: 10.1371/journal.pone.0047853

Qiu Y, Dayrit JK, Davis MJ, Carolan JF, Osterholzer JJ, Curtis JL, Olszewski MA. Scavenger Receptor A modulates the immune response to pulmonary *Cryptococcus neoformans* infection. *J Immunol*. 2013 Jul 1;191(1): 238-248. Epub 2013 Jun 3.